

Stars Notes

Sarafina Nance
Graduate Student
Astrophysics
UC Berkeley

1 Spectral Features

1.1 Absorption Lines

Most stars are surrounded by outer layers of gas that are less dense than the core ($\rho_{outer} < \rho_{core}$). The photons emitted from the core cover all frequencies ν (and energies). Photons of specific frequency can be absorbed by electrons in the diffuse outer layer of gas, causing the electron to change energy levels. Eventually the electron will de-excite and jump down to a lower energy level, emitting a new photon of specific frequency. However, the direction of this re-emission is random, so the chance of the re-emitted photon travelling along the same path as the original incident photon is very small. **The net effect is that the intensity of light at the wavelength of that photon will be less in the direction of an observer and the resultant spectrum will show dark absorption lines.**

2 Stellar Timescales

Timescales just measure when the internal processes of stars come to equilibrium. There are 4 important timescales:

Dynamical Timescale Suppose the internal pressure of the sun were suddenly removed. The outer radius, R , would collapse under gravity according to

$$\frac{d^2 R}{dt^2} = \frac{-GM_{\odot}}{R^2(t)}$$

where $R(0) = R_{\odot}$ and $\frac{dR}{dt}(0) = 0$.

The radius would shrink to zero after an elapsed free-fall time:

$$t_{ff} = \frac{\pi}{\sqrt{8}} \left(\frac{R_{\odot}^3}{GM_{\odot}} \right)^{1/2}$$

Dimensional analysis gives a similar result: it is clear that the collapse time should involve the initial surface gravity $g_{\odot} \equiv \frac{GM_{\odot}}{R_{\odot}^2}$ and radius R_{\odot} in the combination $\sqrt{R_{\odot}/g_{\odot}}$. Ignoring all dimensionless factors of order unity, the dynamical time is therefore:

$$t_{dyn} = \left(\frac{R_{\odot}^3}{GM_{\odot}} \right)^{1/2} \approx 1600 \text{ s}$$

in terms of the mean density:

$$t_{dyn} = \frac{1}{\sqrt{G\bar{\rho}}}$$

While the sun is in no such danger of sudden collapse, this is the characteristic period on which the solar interior vibrates in response to small mechanical disturbances such as solar flares, convection, or even the impacts of in-falling comets. It is roughly the time required for a sound wave to cross the sun.

Collisional (Microscopic) Timescale Photons created in the core of the sun scatter many times on their way out to the surface; actually they are absorbed and re-emitted more than scattered, but never mind that for now. The mean-free path between scatterings is $\lambda = (ne\sigma)^{-1}$, where n_e is the number of electrons per unit volume, and σ is the scattering cross section per electron. Since the sun is mostly hydrogen, $n_e \approx \rho/m_H$. The mass density averaged over the volume of the sun is:

$$\bar{\rho}_{\odot} = \frac{3M_{\odot}}{4\pi R_{\odot}^3}$$

(similar to that of the human body!), hence $n_e \approx 10^{24} \text{ cm}^{-3}$. The cross section is generally of order the Thomson cross section,

$$\sigma_T = \frac{8\pi}{3} \left(\frac{e^2}{m_e c^2} \right)^2 \approx 6 \times 10^{-25} \text{ cm}^2$$

so $\bar{\lambda} \approx 1 \text{ cm}$. The corresponding collision time is:

$$t_{e\gamma} = \frac{\bar{\lambda}}{c} \approx 10^{-10} \text{ s}$$

It can be shown that the proton-electron and proton-proton collision times are similarly short, or even shorter, compared to t_{dyn} and the other relevant macroscopic timescales discussed

below. Importantly therefore, all regions of the interior quickly relax to local thermodynamic equilibrium (LTE). Thermal equilibrium can never be perfect, however, since the surface, which radiates freely to space, is inevitably colder than the core. The temperature gradient drives an outward flux of heat.

Kelvin-Helmholtz (photon diffusion and thermal) Timescale: The thermal time scale is the time required for the Sun to radiate all its reservoir of thermal energy. **Important time scale: determines how quickly a star contracts before nuclear fusion starts - i.e. sets roughly the pre-main sequence lifetime.**

From the Virial Theorem, in which the thermal energy U is roughly equal to the gravitational potential energy:

$$t_{KH} = \frac{U}{L}$$

Photons escape by a random walk of step length λ . The root-mean-square distance after N steps is $dN = N^{1/2}\lambda$. Setting this distance equal to R_{\odot} gives the typical number of steps needed to travel from center to surface: $N \approx \frac{R_{\odot}^2}{\lambda^2} \approx 10^{22}$. The corresponding photon diffusion time is:

$$t_{diff} = Nt_{e\gamma} \approx 10^{12} \text{ s} \approx 3 \times 10^4 \text{ yr}$$

A related timescale is the time required to radiate the current gravitational binding energy of the sun at its current luminosity; this is the Kelvin-Helmholtz time:

$$t_{KH} = \frac{GM_{\odot}^2/R_{\odot}}{L_{\odot}} \approx 3 \times 10^7 \text{ yr}$$

This is the timescale on which the sun would contract if its nuclear energy sources were turned off. It is much longer than the dynamical time (t_{dyn}) because pressure support is lost only gradually, as heat escapes. It is also significantly longer than the photon-diffusion time above. The reason for the latter is that most of the sun's thermal energy is *stored* in the random motions of electrons and ions rather than photons, even though photons dominate the outward *transport* of energy. Photons carry a larger fraction of the thermal energy of stars more massive than the sun, as will be shown.

Nuclear Timescale: This is just the time scale on which the star will exhaust its supply of nuclear fuel if it keeps burning it at the current rate. This is a reasonable estimate of the main-sequence lifetime of the Sun.

The heat released by fusing a mass ΔM of hydrogen into helium is approximately $0.007\Delta Mc^2$. Therefore the time required to exhaust all the sun's hydrogen at its current luminosity would be:

$$t_{nuc} = \frac{0.007 \Delta M_{\odot} c^2}{L_{\odot}} \approx 10^{11} \text{ yr}$$

The actual lifetime of the sun will be about one tenth of this because its luminosity will increase greatly when it becomes a red giant.

SUMMARY: Stellar structure and evolution are quantitatively predictable in large part because of the disparity of timescales:

$$t_{nuc} \gg t_{KH}, t_{diff} \gg t_{dyn} \gg t_{collisions}$$

When analyzing processes associated with one of these timescales, one can usually ignore the slower processes and assume that the more rapid ones are at equilibrium. Most unsolved problems in stellar theory have to do with breakdown in these assumptions: for example, convection and wind-borne mass loss are departures from dynamical equilibrium that have thermal and nuclear consequences.

3 White Dwarfs

3.1 Gravitational Redshift:

Gravitational redshift tells you the ratio of the star's mass to its radius, M/R . There is another quantity that is measurable from stellar spectra, the surface gravity g of the star (the acceleration experienced by a falling body near the surface). This second quantity tells you the ratio of the object's mass to the square of its radius, $g \approx M/R^2$. Combining the two quantities, one can extract both the object's mass M and its radius R .

In other words, combine the following to find mass M and radius R :

1. Gravitational redshift: M/R
2. Surface gravity: $g \approx M/R^2$

3.2 Spectra:

The dominant factor in the appearance of a star's spectrum is its temperature T_{eff} , not its composition.

Continuity: stars are not perfect blackbodies because some atoms absorb strongly in some wavelength ranges. This causes the emission in these ranges to originate at much higher layers in the atmosphere which are cooler.

With access to surface gravity and effective temperature (the temperature at the photosphere), one can determine key properties such as mass and radius.

3.2.1 Temperature T_{eff} :

By computing the temperature ranges for various atoms and ions, it became obvious that the correct ordering of the letter spectral types is OBAFGKM.

3.2.2 Surface Gravity g :

It can be determined to about 25 – 50% precision through spectroscopy, but this requires diluting a stars light through a spectrograph, meaning the technique is only applicable to relatively bright stars.

Asteroseismology, the measurement of stellar oscillations, is even more precise only about 2% uncertain but also requires the ability to distinguish minute flux variations, and so only the very brightest stars can be studied. This means that while we know the temperatures of a huge number of stars fairly accurately, we only have good measures of surface gravities for a tiny subset.

The shape of a spectral line, the line profile, reflects the conditions at a range of heights so that the average gas velocities $v_{avg,gas}$ at different heights have an effect on the range of wavelengths λ included in the spectral line. The line profiles change shape depending on the surface gravity of the star.

Surface gravity has an important effect on stellar oscillations: the higher the gravity, the faster the rate of oscillations (this is why asteroseismology is able to measure gravity).

For most stars, the only chance we have to infer the surface gravity is based on the analysis of spectral features: lines and continuum.

Generalities of spectral lines:

1. The intensity of a spectral line is related to the number of absorbers, i.e. atoms or ions of the given elements at the lower level of the transition.
2. In Local Thermodynamic Equilibrium (LTE), when only one ionization stage is available, the fraction of ions that can absorb is given by the Saha equation that regulates the ionization case

We know that pressure effects in stellar spectra are very weak if compared to temperature effects; in a few words we can say that, while temperatures span a factor of ten or so from O-M stars, pressure ranges over six orders from dwarfs to supergiants. Nevertheless, this is the only effect that we can measure if we want to have a determination of surface gravity.

Photospheres are comprised of gas so,

$$P = nkT$$

$$F_{grav} = \frac{GMm}{R^2} = g\rho H$$

where H is the pressure scale height and $g = \frac{GM}{R^2}$.
The pressure and gravitational force must balance:

$$P = g\rho H$$

For stars of comparable temperatures, those with higher surface gravities will have higher pressures and vice-versa.

3.3 Surface Temperatures T_{eff}

The surface temperature of a single white dwarf, for a given mass, directly yields its luminosity and hence its evolutionary thermal cooling time (age).

$$T_{eff, \text{ single wd}} \propto L \propto \tau_{cool}$$

This is NOT the case for white dwarfs in CVs.

$$L_S = L_{accg} + L_{shear} + L_{rad} + L_{cool} - L_\nu$$

$$T_{eff} = [L_S / (4\pi R R_{wd}^2 \sigma)]^{1/4}$$

where L_{accg} is the long-term average rate at which the gravitational potential energy is liberated in response to accretion. L_{cool} is the thermal cooling luminosity, L_{rad} is the luminosity due to instantaneously radiated accretion luminosity, L_{shear} is the luminosity resulting from shear mixing (rotational kinetic energy (KE) converted into heat and stored inside the white dwarf eventually to be released as surface luminosity), and L_ν is the neutrino luminosity.

- $T_{surf,eff}$ may not be the intrinsic value independent of accretional heating but instead an upper limit to the baseline T_{eff} value— due to the possible contribution of the accretion disk
- The cooling evolution time τ_{cool} cannot be directly inferred and is a lower limit to the stellar cooling age

3.4 Lagrangian Points L :

The volume of space inside of which matter feels a stronger pull from star 1 than star 2 defines the Roche Lobe for star 1, and the volume of space inside of which matter feels a stronger pull from star 2 than star 1 defines the Roche Lobe for star 2.

The two Roche Lobes for stars in a binary system are approximately teardrop shaped, and they meet at a point known as L_1 , or the first Lagrangian point L_1 . At L_1 , the gravitational force from both stars is exactly equal, so matter can actually go from being bound to one star to the other by passing through the L_1 point.

3.5 Eddington Limit and Super-Eddington Luminosities:

The Eddington luminosity (Eddington limit), is the maximum luminosity a body (such as a star) can achieve when there is balance between the force of radiation acting outward and the gravitational force acting inward.

The maximum luminosity of a source in hydrostatic equilibrium is the Eddington luminosity. If the luminosity exceeds the Eddington limit, then the radiation pressure drives an outflow.

$$L_{Edd} = L_{max} \text{ when } F_{rad,out} = F_{grav,in}$$

The state of balance is called hydrostatic equilibrium (HE).

When a star exceeds the L_{Edd} :

- Intense **radiation-driven** stellar wind from outer layers
 - Most stars have $L < L_{Edd}$, so winds are from less-intense **line absorption**.
- Explains observed luminosity of accreting black holes

$$L_{Edd} = \frac{4\pi GMm_p c}{\sigma_T} \approx 3.2 \times 10^4 \left(\frac{M}{M_\odot} \right) L_\odot$$

m_p appears because in the typical environment for the outer layers of a star, the radiation pressure acts on e^- , which are driven away from the center. Because protons are negligibly pressured by the analog of Thomson scattering, due to their larger mass, there's a slight charge separation and therefore a radially directed electric field, acting to lift the positive charges, which are typically free protons. When the outward electric field is sufficient to levitate the protons against gravity, both electrons and protons are expelled together.

3.5.1 Super Eddington Luminosities:

How do we explain very high mass loss rates (high \dot{M}) (e.g. η Carinae)? Regular, line driven stellar winds can only stand for a mass loss rate of around $\dot{M} \approx 10^{-4} - 10^{-3} M_{\odot}$ per yr, whereas mass loss rates of up $\dot{M} \approx 0.5 M_{\odot}$ per yr are needed to understand the η Carinae outbursts. This can be done with the help of the super-Eddington broad spectrum **radiation-driven** winds.

- Exceeds L_{Edd} for *very short times*, resulting in short and highly intensive mass loss rates:
 - GRB
 - Novae
 - SNe
- Exceeds L_{Edd} for *very long times*:
 - X-ray binaries
 - AGN
- L_{Edd} reduces/cuts off the accretion flow, imposing an Eddington limit on accretion (just like it does on luminosity):
 - CVs (accreting WDs)
 - Accreting neutron stars (NS)

Note: for notes on accretion rates and the fluid equations, check out [Ohio State's Notes on Accretion Flows](#).

4 AGN

An active galactic nucleus (AGN) is a compact region at the center of a galaxy that has a higher than normal luminosity over portions of the electromagnetic spectrum. AGN are the most luminous sources of electromagnetic radiation in the Universe, and their evolution puts constraints on cosmological models. In quasars and other types of AGN, the black hole is surrounded by a gaseous accretion disk. As gas in the accretion disk falls toward the black hole, energy is released in the form of electromagnetic radiation. This radiation can be observed across the electromagnetic spectrum at radio, infrared, visible, ultraviolet, and X-ray, and gamma wavelengths.

The majority of AGN are very distant and show large Doppler shifts. This suggests that active galaxies occurred in the early Universe and, due to cosmic inflation, are receding away from the Milky Way at very high speeds. The observation of AGN at large distances and

their scarcity in the nearby Universe suggests that they were much more common in the early Universe, implying that active galactic nuclei could be early stages of galactic evolution.

4.1 Seyfert Galaxies:

Seyfert galaxies are one of the two largest groups of active galaxies, along with quasars. They have quasar-like nuclei (very luminous, distant and bright sources of electromagnetic radiation) with very high surface brightnesses whose spectra reveal strong, high-ionisation emission lines, but unlike quasars, their host galaxies are clearly detectable. Seyfert galaxies are much closer than quasars.

Seyfert galaxies account for about 10% of all galaxies and are some of the most intensely studied objects in astronomy, as they are thought to be powered by the same phenomena that occur in quasars, although they are **closer and less luminous than quasars**. These galaxies have supermassive black holes at their centers which are surrounded by accretion discs of in-falling material. The **accretion discs are believed to be the source of the observed ultraviolet radiation**. Ultraviolet emission and absorption lines provide the best diagnostics for the composition of the surrounding material.

In a typical Seyfert galaxy, the nuclear source emits at visible wavelengths an amount of radiation comparable to that of the whole galaxy's constituent stars.

Seyfert galaxies have extremely bright nuclei, with luminosities ranging between $10^8 L_{\odot} - 10^{11} L_{\odot}$. Only about 5% of them are radio bright; their emissions are moderate in gamma rays and bright in X-rays. Their visible and infrared spectra shows very bright emission lines of hydrogen, helium, nitrogen, and oxygen. These emission lines exhibit *strong Doppler broadening*, which implies velocities from $500 - 4,000 \text{ km/s}$ and are believed to originate near an accretion disc surrounding the central black hole.

4.1.1 Calculating the mass of the central black hole:

A lower limit can be calculated using the Eddington luminosity. This limit arises because light exhibits radiation pressure. Assume that a black hole is surrounded by a disc of luminous gas. Both the attractive gravitational force F_G acting on electron-ion pairs in the disc and the repulsive force exerted by radiation pressure F_{rad} follow an inverse-square law $1/r^2$. If the $F_G < F_{rad}$, the disc will be blown away by radiation pressure.

4.1.2 Emissions:

Emission lines may come from:

1. The surface of the accretion disc itself

2. Clouds of gas illuminated by the central engine in an ionization cone

The exact geometry of the emitting region is difficult to determine due to poor resolution of the galactic center. However, *each part of the accretion disc has a different velocity relative to our line of sight*, and the faster the gas is rotating around the black hole, the broader the emission line will be. Similarly, an illuminated disc wind also has a position-dependent velocity.

Narrow lines are believed to originate from the outer part, where velocities are lower, while the broad lines originate closer to the black hole. This is confirmed by the fact that the narrow lines do not vary detectably, which implies that the emitting region is large, contrary to the broad lines which can vary on relatively short timescales. Reverberation mapping uses this variability to determine the location and morphology of the emitting region.

1. Calculates the mass of the central black hole
2. Calculates the size of the broad line regions
3. Measures the structure and kinematics of the broad line emitting region by observing the changes in the emitted lines as a response to changes in the continuum
4. Requires the assumption that the continuum originates in a single central source

Bands of emission are:

1. Radio emission – synchrotron emission from the jet
2. Infrared emission – from radiation in other bands being reprocessed by dust near the nucleus
3. Highest energy – inverse compton scattering by a high temp corona near the black hole

Unified models explain the difference between Seyfert I and Seyfert II galaxies as being the result of Seyfert II galaxies being surrounded by obscuring toruses which prevent telescopes from seeing the broad line region. Quasars and blazars can be fit quite easily in this model. The main problem of such an unification scheme is trying to explain why some AGN are radio loud while others are radio quiet. It has been suggested that these differences may be due to differences in the spin of the central black hole.

4.2 Quasars:

A quasar (also known as a QSO or quasi-stellar object) is an extremely luminous active galactic nucleus (AGN). It has been theorized that most large galaxies contain a supermassive central black hole with mass ranging from $10^6 - 10^9 M_{\odot}$. The power radiated by quasars is enormous: the most powerful quasars have $L \approx 10^{41} W$, thousands of times greater than an ordinary large galaxy such as the Milky Way.

The huge luminosity of quasars results from the accretion discs of central supermassive black

holes, which can convert between 6%–32% of the mass of an object into energy, compared to just 0.7% for the p-p chain nuclear fusion process that dominates the energy production in Sun-like stars.

It is now thought that all large galaxies have a black hole of this kind, but only a small fraction have sufficient matter in the right kind of orbit at their center to become active and power radiation in such a way to be seen as quasars.

This also explains why quasars were more common in the early universe, as this energy production ends when the supermassive black hole consumes all of the gas and dust near it. This means that it is possible that most galaxies, including the Milky Way, have gone through an active stage, appearing as a quasar or some other class of active galaxy that depended on the black hole mass and the accretion rate, and are now quiescent because they lack a supply of matter to feed into their central black holes to generate radiation.

4.2.1 Quasar Properties:

- Radiation is partially non-thermal (not black-body)
 - 10% have jets and lobes like radio galaxies
- Extremely high energies (brighter than constituent stars by a factor of 100 from:
 - Fermi acceleration
 - Centrifugal acceleration
- Detectable over entire EM spectrum, but brightest in near-UV
- Strong radio emission from jets of matter moving $\sim c$
- Appear as blazars when viewed downward
 - Regions move away from center faster than c (superluminal expansion)– optical illusion from special relativity.
- Emission lines of: H, He, C, Mg, Fe, and O
 - Atoms range from neutral to highly ionized – makes it highly charged
 - Wide range of ionization \rightarrow gas is highly irradiated (thus not just hot gas created by stars, which can't produce a wide range of ionization).

4.2.2 Re-Ionization:

Oldest known quasars ($z = 6$) indicate that the intergalactic medium at that time was neutral gas. More recent quasars show no absorption region but rather their spectra contain a spiky area known as the Lyman-alpha forest; this indicates that the intergalactic medium has undergone re-ionization into plasma, and that neutral gas exists only in small clouds.

The intense production of ionizing UV radiation is also significant, as it would provide a mechanism for re-ionization to occur as galaxies form. Despite this, current theories suggest that quasars were not the primary source of re-ionization; the primary causes of re-ionization were probably the earliest generations of stars, known as Population III stars (possibly 70%), and dwarf galaxies (very early small high-energy galaxies) (possibly 30%).

Quasars show evidence of elements heavier than helium, indicating that galaxies underwent a massive phase of star formation, creating population III stars between the time of the Big Bang and the first observed quasars.

5 Hydrostatic Equilibrium:

Mass within some radius r is the *mass equation* or the *equation of mass conservation*:

$$\mathcal{M}(r) = \int_0^r 4\pi r^2 \rho \, dr.$$

Imagine we have a differential volume of our star defined by the following:

$$\text{Density} = \rho(r)$$

$$\text{Volume} = V = drdA$$

$$\text{Mass} = dm = \rho(r) \times V = \rho drdA$$

If we ask "what is the Force of gravity acting on this differential volume?",

$$F_{grav} = -\frac{GMdm}{r^2} = -\frac{GM}{r^2} \times \rho(r) drdA$$

But $g = \frac{GM}{r^2}$, so:

$$F_{grav} = -g\rho(r) drdA$$

This gravitational force must be balanced by the force of pressure, where

$$P(r + dr) - P(r) = P_{net}$$

Recall that pressure P is just force per area: $P = \frac{F}{A}$, so $F_P = PA$:

$$F_P = (P(r + dr) - P(r))dA$$

For the star to be in equilibrium, these forces must be balanced:

$$F_{grav} = F_P$$

$$-g\rho(r) drdA = (P(r + dr) - P(r))dA$$

$$-g\rho(r)drdA = dPdA$$

In other words,

$$\boxed{\frac{dP}{dr} = -g\rho(r)}$$

$$\boxed{\frac{dP}{dr} = -\frac{GM}{r^2}\rho(r)}$$

5.1 Dynamical (Free-Fall) Time:

Now, imagine we are not in hydrostatic equilibrium. Let's consider 2 (τ_{ff}) in more detail.

$$\tau_{ff} = \frac{\text{distance}}{\text{velocity}} = \frac{d}{v}$$

The distance d is just the radius of the star R , and the relevant velocity is the escape (free-fall) velocity $v = \sqrt{\frac{2GM}{R^2}}$. Thus,

$$\tau_{ff} = \frac{R}{\sqrt{\frac{2GM}{R^2}}}$$

or:

$$\boxed{\tau_{ff} = \tau_{dyn} = \frac{R^{3/2}}{(2GM)^{1/2}}}$$

This is the free-fall, or dynamical, time. This is the time it takes to re-equilibrate with a force imbalance. Realistically, it is more of an oscillation timescale. For the Sun, $\rho \approx 1\text{g/cm}^3$, so $\tau_{ff} = 1\text{ hr}$.

5.2 Bookkeeping:

5.2.1 The average mass per particle, m :

Neutral H has a single p and single e^- , so $m = m_p + m_e$

Ionized H (H^+) occurs when the atom has lost an e^- and therefore has free p and free e^- . Thus, we need to consider the pressure due to p and e^- separately:

$$P = P_p + P_{e^-} = n_p k_B T + n_{e^-} k_B T = 2n k_B T$$

$$\frac{dP}{dz} = 2k_B T \frac{dn}{dz} = -(\rho_p g + \rho_{e^-} g) = -(m_p + m_{e^-})ng \approx -m_p ng$$

$$\frac{dn}{dz} = -\frac{m_p gn}{2k_B T} = \frac{-mgn}{k_B T} \implies m = \frac{m_p}{2}$$

Briefly consider charge neutrality. Hydrostatic equilibrium for p and e^- is shown by:

$$\frac{dP_p}{dz} = -nm_p g + neE, \quad \frac{dP_{e^-}}{dz} = -nm_{e^-} g - neE$$

Adding these,

$$2k_B T \frac{dn}{dz} = -(m_p - m_{e^-})gn$$

Subtracting these,

$$2eE = (m_p - m_{e^-})g$$

E does not contribute to hydrostatic equilibrium, but it does maintain charge neutrality.

5.2.2 Mass fractions of e^- and p :

Let's define the mean molecular weight μ to handle the average mass per particle. Consider the gas pressure due to ions: $P_{ions} = \sum n_i k_B T$. We can write n_i in terms of the total mass density: $n_i = \frac{X_i \rho}{A_i m_p}$, where A_i is the atomic mass and X_i is the mass fraction of ion i . Thus,

$$P_{ions} = \frac{\rho}{m_p} k_B T \sum \frac{X_i}{A_i} = \frac{\rho}{\mu_{ion} m_p} k_B T$$

where

$$\frac{1}{\mu_{ion}} = \sum \frac{X_i}{A_i}$$

Now, consider electrons:

$$P_{e^-} = n_{e^-} k_B T = \frac{\rho}{\mu_{e^-} m_p} k_B T$$

Here, $n_{e^-} = \sum Z_i n_i$, where Z_i is the number of electrons per element/ion, and $\frac{1}{\mu_{e^-}} = \sum \frac{Z_i X_i}{A_i}$. The total pressure is thus:

$$P = P_{ion} + P_{e^-} = \frac{\rho}{\mu m_p} k_B T$$

where $\frac{1}{\mu} = \frac{1}{\mu_{ion}} + \frac{1}{\mu_{e^-}}$

For pure H: $\mu_{ion} = \mu_{e^-} = 1 \implies \mu = 1/2$.

For pure He: $\mu_{ion} = 4, \mu_{e^-} = 2 \implies \mu = 4/3$

Redshift zero cosmic composition is $\sim 75\%$ H, $\sim 23\%$ He, and $\sim 2\%$ other $\implies \mu \approx 0.62$.

6 Virial Theorem:

The Virial Theorem states that, for a stable, self-gravitating, spherical distribution of equal mass objects (stars, galaxies, etc), $KE_{tot} = -\frac{1}{2}PE_{grav}$.

We can derive the Virial Theorem for stars using hydrostatic equilibrium: $\frac{dP}{dr} = -\frac{GM}{r^2}\rho(r)$. Let's multiply HE $\times 4\pi r^3 dr$ and integrate:

$$\text{RHS: } -\rho \frac{GM_r}{r^2} \times 4\pi r^3 dr \implies -\int_0^R 4\pi r^2 \rho dr \cdot \frac{GM_r}{r^2} = -\int_0^M \frac{GM_r}{r} dM_r = U$$

$$\text{LHS: } 4\pi r^3 \frac{dP}{dr} dr = \frac{d}{dr} \left((4\pi r^3 P) - (3 \cdot 4\pi r^2 P) \right) \implies 4\pi r^3 P \Big|_0^R - 3 \int_0^R 4\pi r^2 P dr = -3\langle P \rangle V$$

by integration by parts. Thus,

$$U = -3\langle P \rangle V$$

To calculate the relation $E_{tot} = U + K = -3\langle P \rangle V + KE$, we need to relate K , P , and V (recall stat-mach and thermo). Recall that $P_{ideal\ gas} = nKT$, so $\frac{K}{V} = \frac{3}{2}nKT \implies P = \frac{2K}{3V}$. Thus, we can calculate the pressure due to the collisions of particles with a surface as a force:

$$F = P \cdot A = \frac{\Delta\rho}{\Delta t}$$

where $\frac{\Delta\rho}{\Delta t} = nAv_x\rho_x$. Thus,

$$P = nv_x\rho_x = \frac{1}{3}n\langle\rho v\rangle$$

For non-relativistic particles, $\rho = mv$, so:

$$P = \frac{2}{3}n\langle\frac{1}{2}mv^2\rangle = \frac{2}{3}\frac{K}{V}$$

plugging into $U = -3\langle P \rangle V$

$$\begin{aligned} \implies U &= -2K \\ \implies E_{tot} = U + K &= \frac{U}{2} = -K \end{aligned}$$

For relativistic particles (photons), $E = \rho c$, so:

$$\begin{aligned} P &= \frac{1}{3}n\langle\rho c\rangle = \frac{1}{3}\frac{K}{V} \\ \implies U &= -K \\ \implies E_{tot} = U + K &= 0 \end{aligned}$$

6.1 Example case:

Consider the following star:

- Non-relativistic star, such that $E_{tot} = \frac{U}{2} = -K$
- No internal source of energy (fusion), but has a temperature T , and thus radiation with luminosity L
- Energy of star is decreasing because of L , so $\implies |E_{tot}|$ is increasing
- Assuming the star remains in hydrostatic equilibrium, K increases, and T increases. It follows that $|U|$ increases and R decreases

This process is called Kelvin-Helmholtz contraction (KH contraction). The timescale is:

$$\tau_{KH} \sim \frac{|E_{tot}|}{L} = \frac{|U|/2}{L}$$

For the Sun, $\tau_{KH} \approx 3 \times 10^7$ yr. Now, consider a star that has a little too much fusion or energy generation:

$$|E_{tot}| = \downarrow K \text{ and } \downarrow T, \quad |U| \downarrow \text{ and } R \uparrow$$

Extra energy is used to maintain hydrostatic equilibrium, which causes temperature $T \downarrow$ and radius $R \uparrow$. We see that stars are stable. More fusion leads to an increase in energy which, due to hydrostatic equilibrium, causes a drop in temperature and less fusion. Stars have self-regulating and stable fusion (assuming everything doesn't happen too fast and there's time to adjust).

6.2 When is P_{rad} important?

Let's use the Virial Theorem to estimate the temperature inside of a star. We'll then plug that temperature into the equation for hydrostatic equilibrium, and solve for P_{rad} .

$$K = \frac{|U|}{2} \sim \frac{GM^2}{2R}$$

$$K = \frac{3}{2}k_B T \cdot \frac{M}{\mu m_p}$$

(for an ideal gas).

$$\implies k_B T \sim \frac{GM\mu m_p}{3R}$$

For the Sun, $T \approx 5 \times 10^6$ K. (Whereas $T_{eff} \approx 5800$ K and $T_c \approx 1.5 \times 10^7$ K.)

We can use this to estimate when radiation pressure is important in a star:

$$\frac{dP_{rad}}{dr} \geq \rho \frac{GM_r}{r^2}$$

$$\implies P_{rad} \geq \frac{GM^2}{R^4}$$

We also know that $P_{rad} \sim \frac{1}{3}aT^4 \sim \frac{1}{3}a\left(\frac{GM\mu m_p}{3k_B R}\right)^4$. So, it's important if:

$$M \geq 10\left(\frac{k_B^4}{aG^3\mu^4 m_p^4}\right)^2 \sim 100M_\odot$$

Most stars are not this massive. **Gas pressure is generally more important!**

7 Energy Transport:

We're interested in 3 main modes of energy transport in stars: 1) Radiation; 2) Conduction; 3) Convection.

7.0.1 Flux F :

Let's zoom into a small scale where we aren't worried about random walks— particles move in straight lines. We define the mean free path, l , as the distance particles travel before colliding/scattering and exchanging energy.

$$l = \frac{1}{n\sigma}$$

where σ is the cross section of collision/scattering, and n is the number density of scatterers. Imagine you have cool material falling, and hot material rising. What is the flux passing through the line where the cool material meets the hot material?

$$F = F_{down} - F_{up} = \frac{1}{6}vU(x-l) - \frac{1}{6}vU(x+l)$$

where v is the velocity and U is the volumetric energy density.

$$F = \frac{1}{6}\left[U(x) - \frac{dU}{dx}l\right] - \frac{1}{6}\left[U(x) + \frac{dU}{dx}l\right]$$

$$\implies F = -\frac{1}{3}\frac{dU}{dx}lv$$

Since we care about the temperature gradient, let $\frac{dU}{dx} = \frac{dU}{dT}\frac{dT}{dx}$:

$$\implies F = -\frac{1}{3}lv\frac{dU}{dT}\frac{dT}{dx} = \mathcal{X}\frac{dT}{dx}$$

where \mathcal{X} is the thermal diffusivity.

7.0.2 Example:

Consider an ideal gas of particles in an ionized stellar interior. Assume $P_{gas} \gg P_{rad}$, and $U_{gas} \gg U_{rad}$.

$$U = \frac{3}{2}nk_B T \implies F \approx \frac{1}{2}lvnk_B \frac{dT}{dx} \approx \frac{1}{2} \frac{vk_B}{\sigma} \frac{dT}{dx}$$

Since we are dealing with Coulomb scattering, we want to estimate a Coulomb cross-section. If we assume significant deflection for $k_B T \approx e^2/b$,

$$\sigma \sim \pi b^2 \sim \frac{\pi e^4}{(k_B T)^2} \ln \left(\frac{b_{max}}{b_{min}} \right)$$

Now, we can estimate \mathcal{X} for an ionized ideal gas:

$$\mathcal{X} \approx \frac{1}{2} \frac{k_B v}{\sigma} \approx \frac{1}{2} \sqrt{\frac{k_B T}{m}} \cdot \frac{(k_B T)^2}{\pi c^2} \cdot k_B \propto \frac{T^{5/2}}{m^{1/2}}$$

This dependence on $m^{-1/2}$ implies that electrons dominate the flux.

Lastly, the total power/luminosity flowing through the sphere can be approximated as:

$$L = 4\pi r^2 F = -4\pi r^2 \mathcal{X} \frac{dT}{dr} \sim 4\pi R T \mathcal{X} \sim 10^{-4} \left(\frac{R}{R_\odot} \right) \left(\frac{T}{10^7 \text{ K}} \right)^{7/2}$$

7.1 Radiation:

A more general expression for flux F is: $\vec{F} = -\frac{1}{3}lv \frac{dU}{dT} \vec{\nabla} T$. For photons, $U = aT^4$, $v = c$, and σ is the photon-matter cross-section, so:

$$\vec{F}_{rad} = -\frac{1}{3}lc \vec{\nabla} aT^4 = lc \vec{\nabla} P_{rad}$$

since $P_{rad} = \frac{1}{3}aT^4$.

$$\implies \vec{F}_{rad} = -\frac{4}{3}l \vec{\nabla} \sigma_{SB} T^4 = \mathcal{X} \vec{\nabla} T$$

where $\mathcal{X} = \frac{4}{3}claT^3$.

7.1.1 Opacity:

Opacity measures how effectively a microscopic process of absorption or scattering reduces radiation traveling along a line of sight. Absorption is the destruction of photons when they converted into other forms of energy. Scattering is the absorption of photons coming from one direction that are then re-emitted into other directions, reducing the amount of radiation along a given line of sight. Scattering can either be a continuum process, such as *Compton Scattering*, or a line process, such as *photo-excitation of electrons* from a ground state to an

excited state that then fall back into that same ground state.

We consider the radiative flux incident on a slab of gas of a given density and how the opacity reduces the outgoing flux along the line of sight. The amount of flux exiting the slab depends on the width of the slab ds , the density ρ , and the *effectiveness of the absorption/scattering* which we will call the opacity κ . Each of these factors reduces the amount of radiation that can flow through the slab and therefore the flux is reduced.

$$dF = -\kappa\rho F ds$$

$$\frac{dF}{ds} = -\kappa\rho F$$

Many absorption and emission processes are *frequency dependent* and *anisotropic*, and therefore we transform this flux into a specific intensity I_ν . We also can equate the product of opacity κ and density ρ to the absorption coefficient α_ν to obtain a similar form as the Radiative Transfer Equation where there is assumed to be no emission:

$$\frac{dI}{ds} = -\alpha_\nu I$$

$$\alpha_\nu = \kappa_\nu \rho$$

In general, opacity has a power law dependence on both the density of the gas as well as its temperature.

$$\kappa \simeq \kappa_0 \rho^n T^s$$

Typically κ has a dependence on ρ , T , and composition. Let's look at a few interesting cases:

7.1.2 Electron (Thompson) Scattering:

Case where the photon scatters off of a free electron e^- . Requires sufficient ionization (lots of e^-), so it decreases rapidly for temperatures below the ionization temperature ($\sim 10^4$ K for H and $\sim 5 \times 10^4$ K for He).

$$\kappa_{e^-} = 0.2(1 + X) \text{ cm}^2/\text{g}$$

where X is the hydrogen mass fraction. It is also less important when there are a lot of heavy elements. We see that $n = s = 0$.

7.1.3 Rosseland Mean Opacity and Free-Free Absorption:

A free electron can also gain energy during a collision with an ion by absorbing a photon. This is free-free absorption (requires ions and free e^-).

Theorem 1. *Bremsstrahlung Radiation occurs when an electron passing close to an ion feels an acceleration. An accelerating charge produces radiation. This is free-free emission, also called Bremsstrahlung. It's important at high temperatures, when the plasma is highly ionized.*

A free electron passing an ion can emit or absorb radiation while it is close enough. At temperature T , thermal velocity v is:

$$\frac{1}{2}m_e v^2 \approx kT$$

and the time they are close enough will be proportional to:

$$t \propto v^{-1} \approx T^{-1/2}$$

For plasmas in thermodynamic equilibrium, we can take a flux-weighted mean opacity called the Rosseland mean opacity. Often this opacity is represented with its absorption coefficient counter-part:

$$\begin{aligned} \alpha_R &= \kappa_R \rho \\ \implies \kappa_R &= \alpha_R / \rho = \sigma / m \end{aligned}$$

if the mean free path is $l = \frac{1}{n\sigma} = \frac{1}{\kappa\rho}$, where σ and ρ are frequency-averaged quantities. The averaged κ_R is the Rosseland mean opacity:

$$\frac{1}{\alpha_R} = \frac{\int_0^\infty \frac{1}{\alpha_R} \frac{\partial B_\nu(T)}{\partial \nu} d\nu}{\int_0^\infty \frac{\partial B_\nu(T)}{\partial \nu} d\nu}$$

or:

$$\frac{1}{\kappa} = \frac{\int_0^\infty \frac{1}{\kappa\nu} \frac{\partial B_\nu}{\partial \nu}}{\int_0^\infty \frac{\partial B_\nu}{\partial \nu}}$$

An example of a Rosseland mean opacity κ_R is Kramers Opacity $\kappa_{R,ff}$. For this opacity we assume that we are dominated by free-free absorption.

Kramer's Opacity, $\kappa_{R,ff}$, is relevant when we are dominated by free-free absorption, i.e. when the temperature T of the plasma is hot enough to ionize most electrons e^- while still having a low enough T for those e^- to be pulled in by the proton's electron potential well.

If the density is ρ , the number of systems able to participate n is:

$$n \propto \rho T^{-1/2}$$

A single system has an absorption coefficient proportional to $Z^2 \nu^{-3}$, where Z is the charge number of the ion. Then,

$$\kappa_\nu \propto Z^2 \rho T^{-1/2} \nu^{-3}$$

Most absorption happens near the peak of $B_\nu(T)$, so since $\nu_{max} \sim T$, an intensity-weighted integral over frequency gives Kramer's Law:

$$\boxed{\kappa_{R,ff} \propto \rho T^{-7/2}}$$

More specifically,

$$\kappa_{R,ff} \approx 10^{23} \frac{\rho Z_c^2}{\mu_e \mu_{ion}} T^{-7/2} \text{ cm}^2/\text{g}$$

where Z_c is the average nuclear charge. Note that $\mu_e \rightarrow \infty$ when no electrons are present. This is a form of Kramer's opacity: $n = 1, s = 7/2$.

7.1.4 Bound-Free and Bound-Bound Absorption:

Case where a bound electron absorbs a photon and either escapes the atom or changes energy levels. Typically drops off for $T < 10^4$ K, since most photons cannot fully ionize atoms (for Bound-Free).

$$\begin{aligned}\kappa &\approx 4 \times 10^{25} Z(1 + X)\rho T^{-7/2} \text{ cm}^2/\text{g} \\ \kappa &\approx 4 \times 10^{22} (X + Y)\rho T^{-7/2} \text{ cm}^2/\text{g}\end{aligned}$$

where $X, Y,$ and Z are the hydrogen, helium, and metal mass fractions, respectively. This is a form of Kramer's opacity, $n = 1, s = 7/2$.

7.1.5 H^- Opacity:

Case where bound-free transitions and bound-bound transitions occur in H^- . Requires neutral H and free e^- , which typically only coexist with high enough abundances when there are sufficient metals and T is high enough to ionize the metals, but not too high as to ionize all of the H^- (3000 K – 8000 K).

$$\kappa_{\text{H}^-} \approx 2.5 \times 10^{-31} \left(\frac{Z}{0.02} \right) \rho^{1/2} T^9 \text{ cm}^2/\text{g}$$

Note that $n = 1/2$ and $s = -9$. This is important in **stellar atmospheres**.

7.1.6 Other Sources of Opacity:

Below temperatures of ~ 3000 K, molecules and small grains become the primary opacity source. This is important in **low-mass stars and brown dwarfs**. The plot below shows the Rosseland Mean Opacity, or the combination of these cases:

7.1.7 Photon Flux:

Now, let's consider the flux due to electrons and the flux due to photons:

$$\begin{aligned}\frac{F_{\text{rad}}}{F_{e^-}} &= \frac{\mathcal{X}_{\text{rad}}}{\mathcal{X}_{e^-}} = \frac{aT^3 \cdot c \cdot 1 / (n\sigma_{\gamma-e^-})}{k_B \cdot v_{e^-} \cdot / \sigma_{e^-i}} = \frac{aT^4 \cdot c \cdot 1 / \sigma_{\gamma-e^-}}{nk_B T \cdot v_{e^-} \cdot / \sigma_{e^-i}} \\ \frac{F_{\text{rad}}}{F_{e^-}} &= \frac{P_{\text{rad}}}{P_{\text{gas}}} \cdot \frac{c}{v_{e^-}} \cdot \frac{l_{\gamma}}{l_{e^-}}\end{aligned}$$

But $\frac{P_{\text{rad}}}{P_{\text{gas}}} \ll 1, \frac{c}{v_{e^-}} \gg 1, \frac{l_{\gamma}}{l_{e^-}} \gg \gg 1$, so **photons dominate the flux**. We also see this when we compare the Thomson cross-section (collisions between photons and electrons) and the Coulomb cross-section (collisions between electrons and ions):

$$\sigma_T = \frac{8\pi}{3} \left(\frac{e^2}{m_e c^2} \right)^2 \approx 0.6652 \times 10^{42} \text{ cm}^2$$

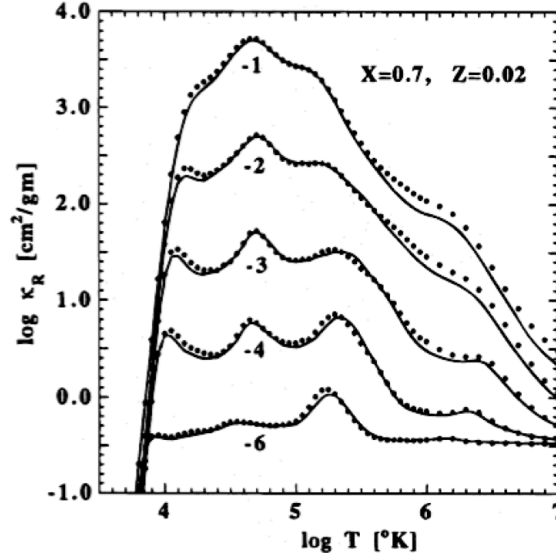


Figure 1: The Rosseland Mean Opacity curve for free-free and bound-free cases. Note that H^- dominates for $T < 10^4$ K, Kramer's dominates for high ρ and $T > 10^4$ K, and e^- scattering dominates for low ρ and $T > 10^4$ K. The numbers below each curve are $R = \log(\rho/T_6^3)$. So, opacity is lower for lower densities ($\kappa \downarrow$ as $\rho \downarrow$).

$$\Rightarrow \frac{\sigma_T}{\sigma_{Coulomb}} = \left(\frac{k_B T}{m_e c^2} \right)^2 / \ln \Lambda \leq 10^{-6}$$

Now, let's estimate the luminosity of a star where the flux is dominated by photons that scatter via Thomson scattering! We also assume $P_{gas} \gg P_{rad}$:

$$F_{rad} = -\frac{4}{3} c a T^3 \frac{dT}{dr} = -\frac{4}{3} \frac{c}{n_e \sigma_T} \frac{dT}{dr}$$

$$\Rightarrow L \sim 4\pi R \cdot \frac{caT^4}{n_e \sigma_T}$$

But $n_e \sim \frac{\rho}{\mu_e m_p} \sim \frac{M}{4R^3 \mu_e m_p}$ and $T \sim \frac{GM\mu m_p}{3k_B R}$:

$$\Rightarrow L \sim \frac{ca(\mu m_p)^4 \mu_e m_p G^4 M^3}{\sigma_T k_B^4} \sim 10^{38} \left(\frac{M}{M_\odot} \right) \text{ erg/s}$$

$$\Rightarrow L \sim M^3 \mu^4 \mu_e$$

We find that a star's luminosity is dependent on a photon's ability to random walk, which is decided by the stellar mass and composition. Recall that for He, M and μ_e are higher than they are for H. This means that stars grow brighter as they fuse $\text{H} \rightarrow \text{He}$.

Here is a relation that is good to know as a rule of thumb:

$$\frac{T_{eff}}{T_c} \sim \left(\frac{l}{L} \right)^{1/4}$$

For the Sun, $l \sim 1$ cm and $L \sim R_\odot \sim 7 \times 10^{11}$ cm, so

$$T_c \sim 500 \cdot T_{eff} \sim 3 \times 10^6 \text{ K}$$

7.1.8 Eddington Luminosity

Now, let's look at how we can derive the Eddington Luminosity (L_{edd}) and polytropic equation of state by considering P_{rad} .

$$F = -cl \frac{dP_{rad}}{dr} = -\frac{c}{\kappa\rho} \frac{dP_{rad}}{dr} = \frac{L_r}{4\pi r^2}$$

$$\implies \frac{dP_{rad}}{dr} = \frac{-\kappa\rho}{c} \frac{L_r}{4\pi r^2}$$

Divide by the hydrostatic equilibrium equation $\frac{dP}{dr} = -\rho \frac{GM_r}{r^2}$:

$$\frac{dP_{rad}}{d\rho} = \frac{L_r \kappa}{4\pi G M_r c} = \frac{L_r}{L_{edd}(r)}$$

where L_{edd} is the Eddington luminosity,

$$L_{edd} = \frac{4\pi G M_r c}{\kappa} = 1.3 \times 10^{38} \text{ erg/s} \left(\frac{M}{M_\odot} \right) \left(\frac{\kappa \text{ cm}^2}{0.4 \text{ g}} \right)^{-1}$$

$$\implies L_{edd} = 3 \times 10^4 L_\odot \left(\frac{M}{M_\odot} \right) \left(\frac{\kappa \text{ cm}^2}{0.4 \text{ g}} \right)^{-1}$$

So, we see that $L_r \approx L_{edd}$ when $P \approx P_{rad}$, i.e. when the star is almost entirely supported by radiation pressure!

Since $L \propto M^3$ and $L_{edd} \propto M$, $L \sim L_{edd}$ for $M \sim 100 M_\odot$.

7.1.9 Polytropic Equation of State

We now introduce the assumption that $\frac{dP_{rad}}{dP} = \text{constant}$, and $P = P_{rad} + P_{gas}$. For $P_{gas} \propto P_{rad}$, we find $T \propto \rho^{1/3}$. Thus, $P \propto P_{rad} \propto \rho^{4/3}$. We can now solve HE:

$$\frac{dM_r}{dr} = 4\pi r^2 \rho$$

and

$$\frac{r^2}{\rho} \frac{dP}{dr} = -GM_r$$

$$\implies \frac{d}{dr} \left(\frac{r^2}{\rho} \frac{dP}{dr} \right) = 4\pi G r^2 \rho$$

If $P(\rho)$, then we can solve. There is a class of models that assume

$$P = \kappa \rho^\gamma = \kappa \rho^{1+1/n}$$

This is the polytropic equation of state.

- Non-relativistic Fermi gas, fully convective stars/planets: $\gamma = 5/3$, $n = 3/2$
- Relativistic Fermi gas, white dwarfs, and neutron stars: $\gamma = 4/3$, $n = 3$

7.1.10 Lane-Emden Equation:

We use the Lane-Emden Equation to solve for the density profiles of polytropes:

$$\frac{1}{\xi^2} \frac{d}{d\xi} \left(\xi^2 \frac{d\theta}{d\xi} \right) = -\theta^n$$

where $\theta = (\rho/\rho_c)^{1/n}$, $\xi = r/a$, $a = \left(\frac{(n+1)\kappa\rho_c^{(1/n-1)}}{4\pi G} \right)^{1/2}$. This equation has analytic solutions for $n = 0, 1, 5$ and must be solved numerically otherwise.

7.2 Convection:

Understanding of convection in stars stems from *mixing length theory (MLT)*. Assumes parcels of stellar fluid that arise from instabilities move between regions of different heat content and transport heat. The distance a parcel is transported by buoyancy is the mixing length l . It assumes the following:

- Parcel has characteristic length of same order as l
- l is much shorter than any length associated with the structure of the star.
- Parcel is always in pressure equilibrium with its surroundings. Buoyancy time is much greater than the sound crossing time $t_{buoy} \gg t_{sound\ crossing}$
- Acoustic phenomena, like shocks, may be ignored
- T and ρ within and outside of the parcel differ by only a small amount
- Parcel's motion is adiabatic, such that the energy loss timescale is much greater than the buoyancy timescale ($t_{energy\ loss} \gg t_{buoy}$)

7.2.1 Schwarzschild Criterion:

Assume a schematic with external gravity g , a parcel with ρ_p, T_p, P_p, S_p and ρ_*, T_*, P_*, S_* separated a distance δ_r from a parcel below with ρ, T, P, S (the parcel and the background star are the same at this location). At the new position, is $\rho_p < \rho_*$ (unstable) or is $\rho_p > \rho_*$ (stable)?

Recall that $S \propto \ln(P/\rho^\gamma)$ for an ideal gas. Consider the following cases:

(a) $\frac{dS}{dr} < 0 \implies S_* < S, P_p = P_*, \text{ and } S_p = S > S_*. \text{ Thus, } \rho_p < \rho_*$

(b) $\frac{dS}{dr} > 0 \implies S_* > S, P_p = P_*, \text{ and } S_p = S < S_*. \text{ Thus, } \rho_p > \rho_*$

So, the criterion for convection (Schwarzschild Criterion) is that:

$$\boxed{\frac{dS}{dr} < 0}$$

We can express this criterion in terms of T and ρ :

$$\begin{aligned} S &\propto \ln\left(\frac{P}{\rho^\gamma}\right) \propto \ln(\rho^{1-\gamma}T^\gamma) \\ \implies \frac{dS}{dr} &\propto (1-\gamma)\frac{d\ln P}{dr} + \gamma\frac{d\ln T}{dr} < 0 \end{aligned}$$

So, convection sets in iff:

$$\boxed{\frac{d\ln T}{dr} < \frac{\gamma-1}{\gamma} \frac{d\ln P}{dr}}$$

or:

$$\boxed{\left| \frac{d\ln T}{dr} \right| > \frac{\gamma-1}{\gamma} \left| \frac{d\ln P}{dr} \right|}$$

since T and $P \downarrow$ with $\uparrow r$. Now, recall that $P_{rad} \propto T^4$, and $\frac{dP_{rad}}{dP} = \frac{L_r}{L_{edd}(r)}$.

$$\implies \frac{d\ln P_{rad}}{d\ln P} = \frac{4d\ln T}{d\ln P} = \frac{P}{P_{rad}} \frac{L_r}{L_{edd}(r)}$$

The critical gradient $d\ln T/d\ln P$ between radiative and convective transport is thus:

$$\boxed{\frac{1}{4} \frac{P}{P_{rad}} \frac{L_r}{L_{edd}(r)} = \frac{\gamma-1}{\gamma}}$$

If the LHS $>$ RHS, convection is induced. Note that the LHS $\propto \kappa$, so **higher opacity means more likely convection**. Let's consider the following cases:

(a) Sun:

(a) $P/P_{rad} \sim 10^3, L/L_{edd} \approx 4 \times 10^{-5} \frac{\kappa}{\kappa_T}$, and $\gamma = 5/3$.

- (b) Convection sets in where $\frac{\kappa}{\kappa_T} \geq 20$, which occurs around $R \approx 0.7R_\odot$, where $T \leq 2 \times 10^6$ K and $\kappa \geq 10\text{cm}^2/\text{g}$
- (b) Low-mass stars:
- (a) $\rho \uparrow$ and $T \downarrow \implies \kappa \uparrow$
- (b) For $M \leq 0.3M_\odot$, stars on the MS are fully convective.
- (c) High-mass stars:
- (a) $\rho \downarrow$ and $T \uparrow \implies \kappa \downarrow$
- (b) Don't have surface convection like the Sun, but have core convection. Highest-mass stars are fully radiative.

7.2.2 Brunt-Väisälä Frequency

Convective instability can also be derived using linear perturbation theory. We find: $\delta\ddot{r} + N^2\delta r = 0$, where N^2 is the Brunt-Väisälä Frequency. Note that:

$$N^2 = -g \left(\frac{d \ln \rho}{dr} - \frac{1}{\gamma} \frac{d \ln P}{dr} \right) = \frac{g}{c_s} \frac{dS}{dr} = \frac{gm_p}{\kappa} \frac{\gamma - 1}{\gamma} \frac{dS}{dr}$$

For $N^2 > 0$, you get stable oscillations via internal gravity wave (g-waves). For $N^2 < 0$, you get exponential instabilities.

7.2.3 Convective velocity v_c :

We can study the convective velocity v_c by looking at the total energy flux, where $F = KE + E_{thermal}$:

$$F = \frac{1}{2} \rho v_c^2 \cdot v_c + \rho \Delta E \cdot v_c$$

where ΔE is the thermal energy per unit mass difference, $\Delta E = c_p \Delta T$, and ΔT is the temperature difference between blob (parcel) and surroundings. Assuming $l = \alpha H$ (where H is the pressure scale height and $\alpha = 1$), we can derive an expression for v_c :

$$v_c^2 \sim al \sim |N^2| l^2 = \frac{gl^2}{H} \left| \frac{H}{c_p} \frac{dS}{dr} \right| = gH\alpha^2 \left| \frac{H}{c_p} \frac{dS}{dr} \right|$$

$$\implies v_c^2 = \alpha^2 c_s^2 \left| \frac{H}{c_p} \frac{dS}{dr} \right|$$

$$\boxed{\implies v_c = \alpha c_s \left| \frac{H}{c_p} \frac{dS}{dr} \right|^{1/2}}$$

and

$$F_c \sim \frac{1}{2} \rho \alpha^3 c_s^3 \left| \frac{H}{c_p} \frac{dS}{dr} \right|^{-3/2}$$

For the Sun at the base of the convective zone ($R \sim 0.7R_\odot$): $\rho \sim 1 \text{ g/cm}^3$, $T \sim 10^6 \text{ K}$, $c_s \sim 100 \text{ km/s}$, $F_c \sim \frac{L_\odot}{4\pi R_\odot^2}$

$$\implies v_c \sim 30 \text{ km/s} \sim 3 \times 10^{-4} c_s, \left| \frac{H}{c_p} \frac{dS}{dr} \right| \sim 10^{-7} \ll 1$$

The dimensionless entropy gradient is very small, so entropy is approximately constant. Thus, $P \propto \rho^\gamma$ to high accuracy (which means that it's well-modeled by polytropes).

$$\implies \text{Timescale } \tau \sim H/v_c \sim 1 \text{ month}$$

For the Sun in the photosphere:

$$H \sim 10^{-3} R_\odot, v_c \sim 7 \text{ km/s}, \left| \frac{H}{c_p} \frac{dS}{dr} \right| \sim 1$$

$$\implies \text{Timescale } \tau \sim H/v_c \sim 1 \text{ minute}$$

Thus, eddies become smaller near the surface.

7.2.4 Fully Convective Stars:

These are typically stars on the MS that have $M \leq 0.3M_\odot$ and stars that are pre- and post-MS. We saw before that radiative stars where $\sigma = \sigma_T$ dominates have $L \propto M^3$. Let's find the analogous relation for convective stars.

Assuming the star is adiabatic, an ideal gas, and is best described by $n = 3/2$:

$$P \propto \rho^{5/3} \propto \rho^T \\ \implies P \propto T^{5/2}$$

We can now learn about the photosphere of the star:

$$\frac{P_c}{P_{ph}} = \left(\frac{T_c}{T_{eff}} \right)^{5/2}$$

For an $n = 3/2$ polytrope:

$$P_c = 0.77 \frac{GM^2}{R^4} \implies k_B T_c = 0.54 \frac{GM \mu m_p}{R}$$

We can use these to find T_{eff} and L . Note that the photosphere is where $T = T_{eff}$ and $l_{mfp} = \frac{1}{\kappa \rho} = H = \frac{P}{\rho g}$.

$$\implies P_{ph} \approx \frac{g}{\kappa_{ph}} = \frac{GM}{\kappa_{ph} R^2} = \frac{\rho_{ph} k_B T_{eff}}{\mu m_p}$$

$$\begin{aligned} \implies k_B T_{eff} &= k_B T_c \left(\frac{P_{ph}}{\rho_c} \right)^{2/5} = -0.6 \frac{GM\mu m_p}{R} \left(\frac{R^2}{M\kappa_{ph}} \right)^{2/5} \\ &\implies \rho_{ph} \approx \frac{g\mu m_p}{k_B T_{eff} \kappa_{ph}} \end{aligned}$$

For fully convective objects: $\kappa_{ph} = \kappa_{H^-} \propto \rho_{ph}^{1/2} T_{eff}^9$:

$$\begin{aligned} \implies T_{eff} &\approx 4000 \text{ K} \left(\frac{M}{M_\odot} \right)^{1/7} \left(\frac{R}{R_\odot} \right)^{1/49} \\ \implies L &= 4\pi R^2 \sigma T_{eff}^4 = 0.2 L_\odot \left(\frac{M}{M_\odot} \right)^{4/7} \left(\frac{R}{R_\odot} \right)^{102/49} \propto M^{4/7} R^2 \\ \implies T_{eff} &\approx 4000 \text{ K} \left(\frac{L}{L_\odot} \right)^{1/102} \left(\frac{M}{M_\odot} \right)^{7/51} \end{aligned}$$

So, fully convective stars have approximately constant temperatures while they evolve onto the MS via the **Hayashi Track**. Stars evolving on the Hayashi Track undergo Kelvin-Helmholtz contraction.

7.2.5 Kelvin-Helmholtz Contraction of Fully Convective Stars:

Recall $L = -\frac{dE_{tot}}{dt} = \frac{-dU/2}{dt}$. For an $n = 3/2$ polytrope:

$$U = \frac{-G}{7} \frac{GM^2}{R}$$

. For $L = 0.2 L_\odot \left(\frac{M}{M_\odot} \right)^{4/7} \left(\frac{R}{R_\odot} \right)^2 \propto M^{4/7} R^2$:

$$\begin{aligned} \left(\frac{R}{R_\odot} \right) &\approx \left(\frac{2 \times 10^7 \text{ yr}}{t} \right)^{1/3} \left(\frac{M}{M_\odot} \right)^{1/2} \\ \implies R &\propto t^{-1/3} \implies L \propto R^2 \propto t^{-2/3} \end{aligned}$$

So the luminosity due to convection decreases with time. Radiative energy transport takes over when $L_{rad} > L_{conv}$. This occurs around: $t_{rad} \approx 10^6 \text{ yr} \left(\frac{M}{M_\odot} \right)^{-15/7}$. So, lower mass stars spend more time as fully convective and higher-mass stars become radiative more quickly.

8 Fusion:

8.0.1 Basics of fusion:

Let's be explicit about the notation:

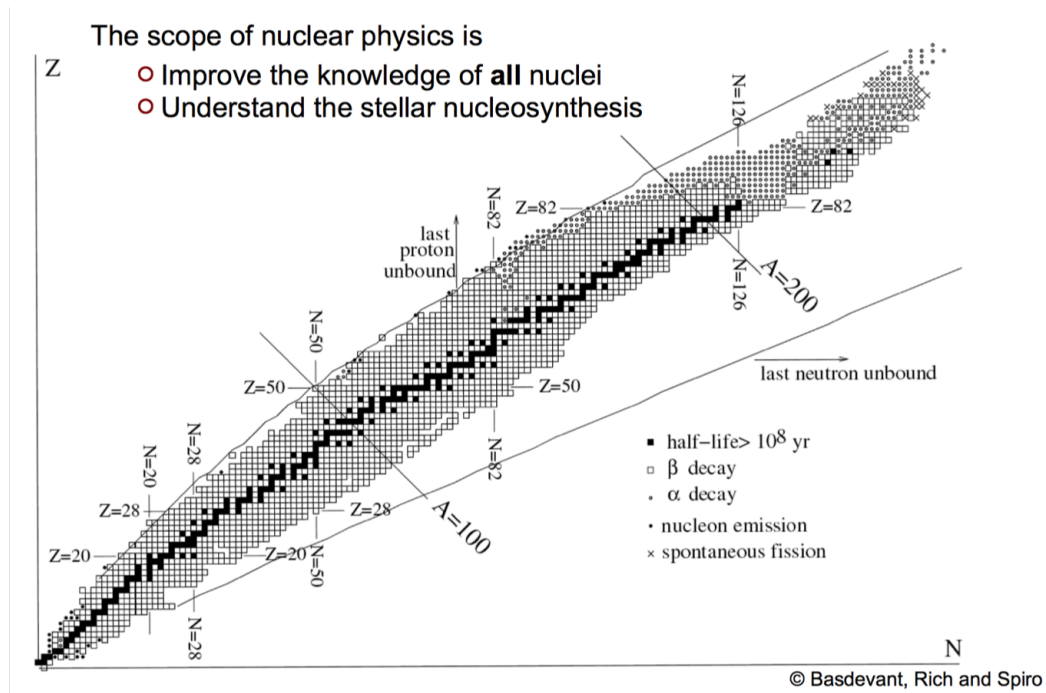


Figure 2: This plot shows the stability of different Z , N pairs. Adding more neutrons for nuclei of higher charges increases stability to radioactivity. If $\#p > \#n$, p decay to n . If $\#n > \#p$, n decay to p . Fermi-Dirac statistics tend to create an equal number of p and n .

Z	proton	$m_p c^2$	938.259 MeV
N	neutron	$m_n c^2$	939.553 MeV
n/a	n/a	$m_n - m_p$	1.3 MeV
n/a	n/a	$m_e c^2$	511 KeV

$$A = Z + N \equiv \text{atomic mass}$$

$$r_n \approx 1.3 \times 10^{-3} \text{ cm} A^{1/3}$$

$$\rho_n = \frac{m_p A}{4/3\pi r_n^3} \sim 2 \times 10^{14} \text{ g/cm}^3$$

Example of Fermi-Dirac statistics (β decay):

$$n \rightarrow p + e^- + \bar{\nu}_e$$

$$p \rightarrow n + e^+ + \nu_e$$

Upon fusing, nuclei release energy equal to the binding energy E_b . For atoms lighter than Fe-56, E_b provides enough energy for subsequent atoms to overcome the Coulomb barrier. For atoms heavier than Fe-56, E_b decreases with A , so subsequent atoms cannot overcome the Coulomb barrier.

The expected lifetime of stars from fusion is:

$$\tau_{\text{fusion}} = \frac{E}{L}$$

For ${}^4\text{He}$, $E_b = 28.3$ MeV and $E_b/A = 7$ MeV. Thus, more generally,

$$E = 28 \text{ MeV} \frac{M_{\odot}}{4m_p} \implies \tau_{\text{fusion}} \sim 10^{11} \text{ yrs}$$

8.1 Coulomb Barrier and WKB Approximation:

Two positively charged nuclei must overcome Coulomb barrier (long range force $\propto 1/r^2$), to reach separation distances where strong force dominates (10^{-15} m, typical size of nucleus). Let's assume a barrier height energy of:

$$E_c = \frac{Z_A Z_B e^2}{r_N}$$

in cgs. Then, the energy of approach is:

$$E = \frac{Z_A Z_B e^2}{r_c}$$

in cgs. Classically, overcoming the barrier requires $k_B T \geq E_c$. This just means that we'd need $T \geq 10^{10} Z_A Z_B$ K, which is **WAY** too high. So, what happens instead?

Clearly, we can't treat this classically. Atoms overcome the barrier and enter the strong force regime thanks to *quantum tunneling*. Tunneling becomes important when the de Broglie wavelength exceeds the distance of closest approach:

$$\begin{aligned} \lambda &\geq r_c \\ \implies \frac{h}{\rho} &\geq \frac{e^2 Z_A Z_B 2m}{\rho^2} \\ \implies \sqrt{mk_B T} &\geq \frac{e^2 Z_A Z_B 2m}{h} \\ \implies T &\geq \frac{4Z_A^2 Z_B^2 e^4 m}{k_B h^2} \\ \implies T &\geq 3 \times 10^7 Z_A Z_B \frac{m}{m_p} \text{ K} \end{aligned}$$

Another important quantity to consider is the fusion cross-section. For a particle passing through a medium containing n target particles per unit volume, the probability that the incoming particle reacts as it travels a distance Δx ,

$$P(\text{react}) = \sigma n \Delta x$$

The cross-section σ is composed of a factor dependent on the nuclear physics of fusion (strong/weak forces, mostly empirical) and a factor that describes the probability of penetration due to quantum tunneling. Let's investigate this further by solving the Schrodinger Equation:

$$\frac{-\hbar^2}{2m}\nabla^2 + \frac{e^2 Z_A Z_B}{r}\Psi = E\Psi$$

Let $\Psi(r, \theta, \phi) = Y_{ml}(\theta, \phi) f_l(r) = E f_l(r)/r$:

$$\left[\frac{-\hbar^2}{2m}\nabla^2 + \frac{e^2 Z_A Z_B}{r} \right] f_l(r) = E f_l(r)$$

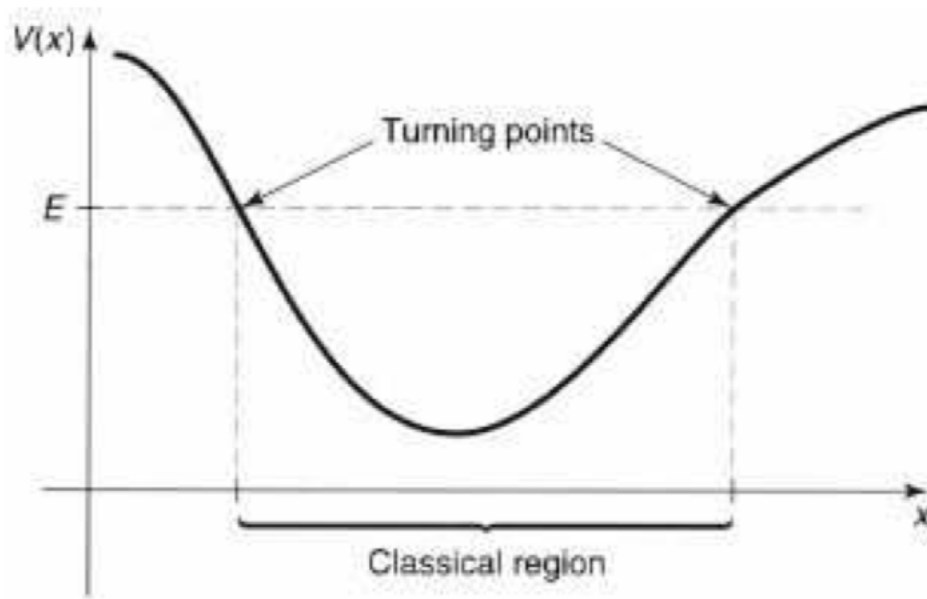
If we assume $l = 0$, we get:

$$\frac{d^2 f}{dr^2} + g(r)f = 0$$

where $g(r) = \frac{2m}{\hbar^2} \left(E - \frac{e^2 Z_A Z_B}{r} \right) < 0$. We must now consider the **WKB short wavelength solution**, which is valid if λ is small compared to the lengthscale over which the potential is changing.

The WKB approximation is a method for obtaining an approximate solution to a time-independent one-dimensional differential equation, in this case the Schrodinger Equation. Its principal applications for us will be in calculating bound-state energies and tunneling rates through potential barriers.

Note that both examples involve what is called the classical turning point, the point at which the potential energy V is approximately equal to the total energy E . This is the point at which the kinetic energy equals zero, and marks the boundaries between regions where a classical particle is allowed and regions where it is not.



Classically, the particle would be confined to the region where $E \geq V(x)$.

$E > V$: a classically allowed region The Schrodinger Equation equation,

$$-\frac{\hbar^2}{2m} \frac{d^2\Psi}{dx^2} + V(x)\Psi = E\Psi$$

can be re-written without approximation as

$$\frac{d^2\Psi}{dx^2} = \frac{-\rho^2}{\hbar^2}\Psi$$

where $\rho(x) = \sqrt{2m(E - V(x))}$. If $E > V$, then $\rho(x)$ is real and one can write $\Psi(x) = A(x)e^{i\phi(x)}$, where A and ϕ are both real functions of x .

Substituting this expression for Ψ into the re-written Schrodinger equation yields:

$$A'' + 2i\phi' A' + iA(\phi'') - A(\phi')^2 = \frac{-\rho^2}{\hbar^2}A$$

The real and imaginary parts of this equation must both hold. After some manipulation, these two equations become

$$A'' = A\left[(\phi')^2 - \frac{\rho^2}{\hbar^2}\right]$$

$$(A^2\phi')' = 0 \implies A = \frac{C}{\sqrt{\phi'}}$$

The first equation cannot be solved in general, leading to the principal approximation of the WKB method.

WKB method: Assume that A varies sufficiently slowly that $A''/A \ll (\phi')^2$ and ρ^2/ϕ^2 .

Let's apply the WKB approximation to our Schrodinger equation. If g is almost constant,

$$\begin{aligned} f &= e^{i(r)} \rightarrow f' = i\phi' f \rightarrow f'' = i\phi'' f - \phi'^2 f \\ &\Rightarrow i\phi'' f - \phi'^2 f + g(r)f = 0 \end{aligned}$$

For $\phi(r) = \sqrt{g(r)}r$ and $\phi'' \approx 0$, $\phi'(r) = \sqrt{g(r)} \rightarrow \int^{r'} \sqrt{g(r)} dr$.

Now, the tunneling probability is $|f(r)|^2 \sim e^{-\tau}$.

$$\begin{aligned} I &= 2 \int_{r_n}^{r_c} \sqrt{|g(r)|} dr = \frac{2\sqrt{2m}}{\hbar} \int_{r_n}^{r_c} \left(\frac{e^2 Z_A Z_B}{r} - E \right)^{1/2} dr \\ I &= \frac{2\sqrt{2mE}}{\hbar} \int_{r_n}^{r_c} \left(\frac{e^2 Z_A Z_B}{Er} - 1 \right)^{1/2} dr = \frac{2\sqrt{2mE} \cdot r_c}{\hbar} \int_{r_n/r_c}^{r_c/r_c} \left(\frac{r_c}{r} - 1 \right)^{1/2} dr \end{aligned}$$

Let $x = r/r_c$

$$\begin{aligned} I &= \frac{2\sqrt{2mE} \cdot r_c}{\hbar} \int_{r_n/r_c}^1 \left(\frac{1}{x} - 1 \right)^{1/2} dx \approx \frac{2\sqrt{2mE} \cdot r_c}{\hbar} \left(\frac{\pi}{2} \right) = \frac{\pi\sqrt{2mE}r_c}{\hbar} \\ &\Rightarrow I = \frac{\pi\sqrt{2mE}r_c}{\hbar} \end{aligned}$$

Note that if we let $E = \frac{\rho^2}{2m}$, $I \sim \frac{r_c}{\hbar/\rho} \sim \frac{r_c}{\lambda}$. **Thus, the tunneling probability only becomes high if $\lambda \geq r_c$.**

$$\Rightarrow I = \frac{2\sqrt{2mE}Z_A Z_B e^2}{E\hbar} = \left(\frac{E_G}{E} \right)^{1/2}$$

The probability of tunneling is thus:

$$I = e^{\sqrt{E_G/E}}$$

where E_G is the Gamow energy, defined as:

$$E_G = \frac{2\sqrt{2mE}Z_A Z_B e^2}{\hbar} \approx 1 \text{ MeV } Z_A^2 Z_B^2 \left(\frac{m}{m_p} \right)$$

The cross-section can be written as a function of E :

$$\sigma(E) = \frac{S(E)}{E} \cdot e^{\sqrt{E_G/E}}$$

where $S(E)$ is the intrinsically nuclear physics part of the cross-section. σ is commonly written in units of ‘‘barns’’ (10^{-24} cm^2). Thus,

$$[S] = \text{barn KeV}$$

At the center of a star, $E \sim 1 \text{ KeV}$. For strong interactions, $S \sim 1 \text{ barn KeV} \rightarrow \sigma \sim 1 \text{ barn} \sim 10^{-24} \text{ cm}^2$. For weak interactions, $S \sim 10^{-22} \text{ barn KeV} \rightarrow \sigma \sim 10^{-22} \text{ barn} \sim 10^{-44} \text{ cm}^2$.

The Gamow Window: Stars are composed of hot gases in which the atoms and molecules are almost completely ionized in the interior (this is plasma). The question of whether fusion reactions can occur in this plasma is primarily one of the ρ , P , and T . The density ρ controls the number of collisions n and the temperature T controls their average energy KT .

The higher the electric charges of the interacting nuclei, the greater the Coulomb repulsive force, hence the higher the kinetic energy and temperature required before reactions occur. Highly charged nuclei are the more massive, so reactions between light elements occur at lower temperature than reactions between heavy elements. But, in other words, classical mechanics prevents the two protons from fusing because they will never have enough energy to overcome the Coulomb repulsion. The energy of the coulomb barrier is:

$$E_C = \frac{Z_A Z_B e^2}{r_0}$$

where r_0 is the radius at which nuclear attraction overcomes Coulomb repulsion, $r_0 \sim 10^{-15}m$. For 2p, $E \approx 1$ MeV. Recall that the mean kinetic energy is proportional to T :

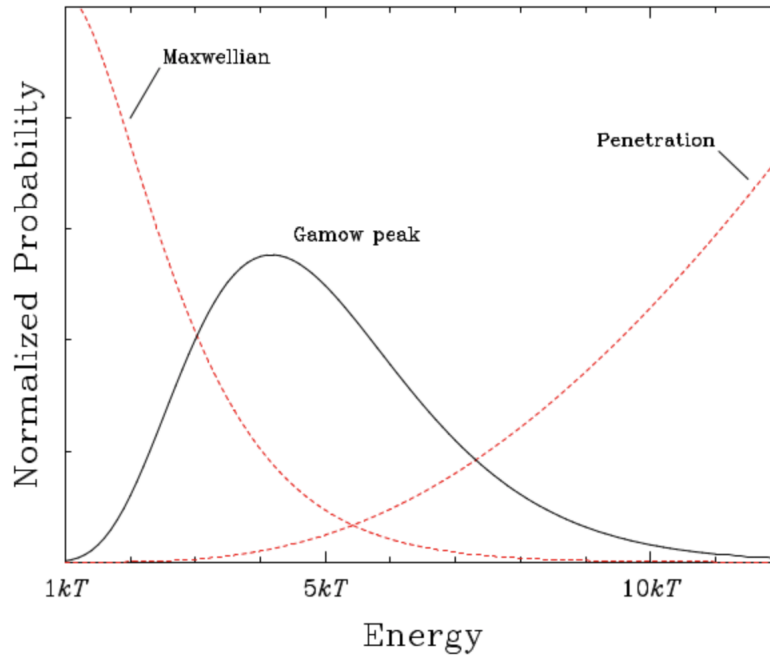
$$E = \frac{1}{2}mv^2 = \frac{3}{2}KT$$

But in the solar core, $T_c \sim 1.5 \times 10^7$ K. This yields $E \sim 10^{-3}E_c$. So, the core isn't hot enough to bring the protons close enough to trigger fusion– it only brings protons within $10^{-3}r_0$ of each other. Thus, the protons aren't close enough by a factor of 10^3 .

Gamow calculated that protons with $E = 3 - 10$ MeV (which there are plenty of in the Sun's core) can overcome the Coulomb barrier (of 1 MeV) through a process of quantum tunneling (or barrier penetration). It is the following constraints that make stars have lifetimes of $\sim 10^9$ years:

1. The low probability of quantum tunneling, along with
2. The need for a weak interaction in order to fuse 2 protons into a deuterium (${}^2\text{H}$, or heavy hydrogen) nucleus

The Coulomb barrier for charged particle reactions and the distribution of velocities implied by the kinetic theory of gases imply **there is a narrow range of energies where nuclear reactions involving charged nuclei occur in stars**. This window is called the Gamow window.



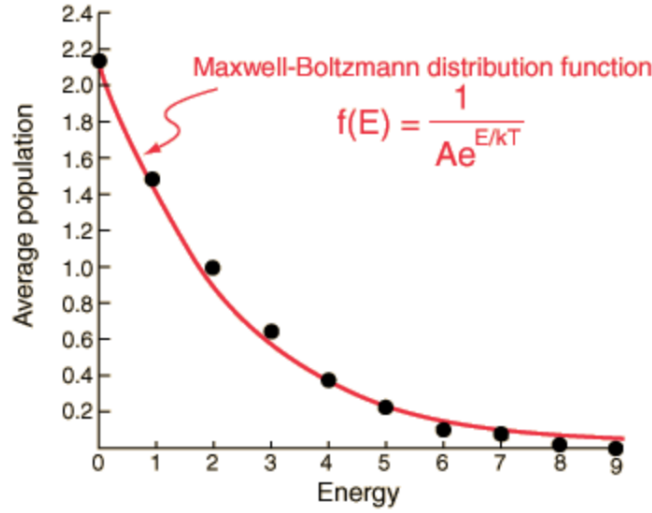
The peak is the product of the two curves decreasing in opposite directions: The probability for penetrating the Coulomb barrier decreases rapidly with decreasing energy ($P_{\text{penetrate barrier}} \downarrow$ with $\downarrow E$ since $E = \lambda\nu$). With a Maxwell-Boltzmann distribution, at a given T , the possibility of having a particle of high KE (\implies high v for the particle behavior) decreases rapidly with increasing energy (because of $E = mc^2$ and mass resists to acceleration, that is, a change in velocity). Put in other words:

$$P_{\text{particle with high KE}} \downarrow \text{with } \uparrow E$$

Gamow peak is:

Peak = Maxwellian distribution \times tunneling probability

$$\text{Peak} \propto e^{-mv^2/2KT} \times e^{-\pi Z_A Z_B e^2 / h\nu E}$$



The area under the Gamow peak determines the reaction rate.

$$A_{\text{Gamow peak}} \propto R$$

where R is the reaction rate. The higher the electric charges q of the interacting nuclei, the greater the repulsive force, hence the higher the E_{kin} and T before reactions occur.

$$\uparrow q \implies \uparrow F_{\text{repulsive}} \implies \uparrow E_{kin} \implies \uparrow T$$

Highly charged nuclei are obviously the more massive, so reactions between light elements occur at lower T than reactions between heavy elements.

To conclude, the sum of these opposing effects produces an energy window for the nuclear reaction: only if the particles have energies approximately in this window can the reaction take place.

Another important quantity to consider is the reaction rate R , or the number of reactions per unit time per unit volume.

$$R \propto \#_{\text{reactions}}/\text{time}/\text{volume}$$

The reaction rate occurs between two types of particles, 1 and 2.

$$R_{12} = n_1 n_2 \langle \sigma v \rangle$$

where $\langle \sigma v \rangle$:

$$\begin{aligned} \langle \sigma v \rangle &= \int d^3v \cdot v \sigma(E) \left(\frac{m_r}{2\pi k_B T} \right)^{3/2} e^{-\frac{1/2 m_r v^2}{k_B T}} \\ &= \left(\frac{2}{k_B T} \right) \frac{1}{\sqrt{\pi m_r}} \int dE \cdot E \sigma(E) e^{-E/k_B T} \\ &= \left(\frac{2}{k_B T} \right) \frac{1}{\sqrt{\pi m_r}} \int dE \cdot S(E) e^{-E/k_B T - \sqrt{E_G/E}} \end{aligned} \quad (1)$$

If we assume $S(E)$ is constant and everything is concentrated at one energy,

$$\langle \sigma v \rangle \propto \int_0^\infty dE \cdot e^{-f(E)} \quad (2)$$

where $f(E) = \frac{E}{k_B T} + \left(\frac{E_G}{E}\right)^{1/2}$. Thus, the reaction rate peaks at an energy E_0 , known as the Gamow peak. E_0 is defined by $f'(E_0) = 0$, which implies:

$$\begin{aligned} E_0 &= \left(\frac{1}{2} E_G^{1/2} k_B T\right)^{2/3} \\ &\approx 5.7 \text{ KeV} \cdot Z_A^{2/3} Z_B^{2/3} T_7^{2/3} \left(\frac{m_r}{m_p}\right)^{1/3} \end{aligned} \quad (3)$$

Now, we can write $f(E) = f(E_0) + \frac{1}{2}(E - E_0)^2 f''(E_0)$, so:

$$\langle \sigma v \rangle \propto e^{-f(E_0)} \int_0^\infty dE \cdot e^{-4(E-E_0)^2/\Delta^2} \quad (4)$$

where $f(E_0) = 3\left(\frac{E_G}{4k_B T}\right)^{1/3}$ and $f''(E_0) = \frac{3}{4}\left(\frac{E_G}{E_0^5}\right)^{1/2}$, and $\Delta \approx 5.1 \text{ KeV} T_7^{5/6} Z_A^{1/3} Z_B^{1/3} \left(\frac{m_r}{m_p}\right)^{1/6} < E_0$. If we consider the E range from $-\infty$ to ∞ , we find:

$$\langle \sigma v \rangle \propto e^{-f(E_0)} \sqrt{\pi} \Delta / 2 \implies \boxed{\langle \sigma v \rangle \approx 2.6 \text{ eV} \cdot S(E_0) \frac{E_G}{(k_B T)^{3/2} m_r^{1/2}} e^{-3\left(\frac{E_G}{4k_B T}\right)^{1/3}}} \quad (5)$$

Now that we know the reaction rate, we can find the energy generated by fusion. Let's use the following units:

$$[\epsilon(\rho, T, \text{composition})] = \text{erg/s/g}$$

Note that

$$L_r = \int_0^r dM_r \cdot \epsilon$$

where $\epsilon_{12} = \frac{Q_{12} r_{12}}{\rho}$, and $\epsilon = \sum \epsilon_{12}$. Here, Q_{12} is the energy released in one reaction. It follows that the proportionalities are:

$$\epsilon \propto \frac{\rho S}{T^{2/3}} e^{-3\left(\frac{E_G}{4k_B T}\right)^{1/3}} \propto \rho^\alpha T^\beta$$

where $\alpha = 1$ for 2-body interactions and $\beta = \frac{d \ln \epsilon}{d \ln T} = \frac{-2}{3} + \left(\frac{E_G}{4k_B T}\right)^{1/3}$.

Let's look at this for the Sun. Relevant quantities:

T	10^7 K
ρ	1 g/cm^3
Q	10 MeV
E_G	$0.5 \text{ MeV (p + p} \rightarrow \dots)$
S	$1 \text{ barn KeV (strong interaction)}$
ϵ	10^{20} erg/s/g

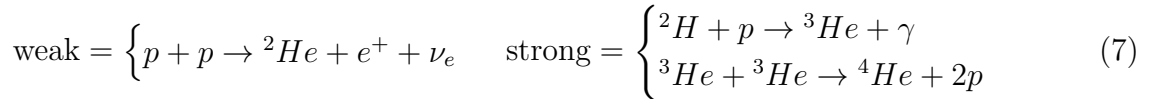
$$L \approx \int dM_r \cdot \epsilon \sim 0.1 M_\odot \cdot \epsilon \sim 10^{53} \text{ erg/s} \sim 10^{19} L_\odot \quad (6)$$

This is WAY too high! That means we could have two solutions:

1. Weak interaction is slow (dominating) step. (p - p chain, $M \leq M_\odot$)
2. Strong interaction is slow step but fusion of p to He uses high- Z catalysts (CNO cycle, $M \geq M_\odot$).

For the Sun, p - p dominates with some CNO present.

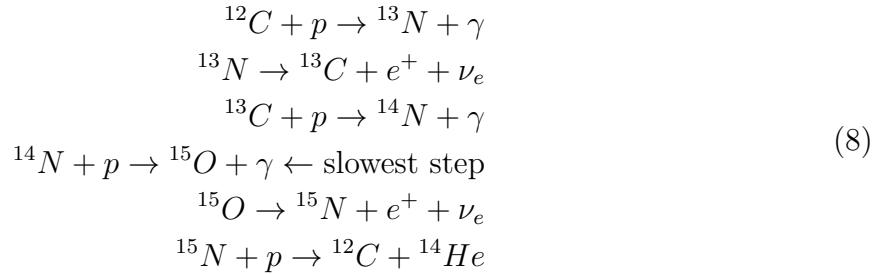
Let's look at the p - p chain:



In this case, the first (weak) step is the slowest. You end up with:

$$\epsilon_{pp} = 5.2 \times 10^5 \text{ erg/s/g} \cdot \frac{\rho X^2}{T_7^{2/3}} e^{-15.7T_7^{-1/3}}$$

Now, let's look at the CNO cycle. Here, $H \rightarrow He$ using CNO as a catalyst.



The slow step in this case gives a different value for $S(E_0)$. You end up with:

$$\epsilon_{CNO} = 4.4 \times 10^{27} \text{ erg/s/g} \cdot \frac{\rho X Z_{CNO}}{T_7^{2/3}} e^{-70.7T_7^{-1/3}}$$

For CNO at $T \sim 10^7$ K, $\epsilon_{CNO} \propto \rho T^{20}$.

In sum, the core temperature is important for determining which mechanism dominates. For $M \geq M_\odot$ (higher T_c), there's mostly CNO. For $M \leq M_\odot$ (lower T_c), there's mostly p - p chain.

8.2 Main Sequence Stars:

Let's recall our relations for luminosity:

L_{rad}	M^3	Thompson scattering dominated
L_{rad}	$M^{5.5} R^{-0.5}$	free-free opacity dominated
L_{conv}	$M^{4/7} R^2$	fully convective
L_{fusion}	$\int dM_r \cdot \epsilon$	overall

Steady-state hydrogen fusion main sequence occurs when $L_{fusion} = L_{rad}/L_{conv}$. Initially, stars are very large and have little-to-no fusion. Luminosity at this point comes from K-H contraction:

$$L_{KH} \approx L_{rad/conv} \rightarrow R \downarrow \rightarrow T_c \uparrow \rightarrow L_{fusion} \uparrow$$

Once $L_{fusion} \approx L_{rad/conv}$, K-H contraction stops. For:

- Lower mass stars ($M \leq M_\odot$), L_{fusion} is mostly $p - p$ fusion
- Higher mass stars ($M \geq M_\odot$), L_{fusion} is mostly CNO fusion

8.2.1 Low Mass Stars on the MS:

Let's derive some scaling relations for low-mass MS stars ($M \sim 0.5M_\odot - 1.0M_\odot$), Assume the star is:

- Gas pressure supported
- Energy transport = radiative transport and free-free opacity
- Fusion = $p - p$ chain.

$$L_{rad} \propto M^{5.5} R^{-0.5}$$

$$L_{pp} \propto M \epsilon_{pp} \propto M^2 R^{-3} \cdot M^{4.5} R^{-4.5} \propto M^{6.5} R^{-7.5}$$

But:

$$L_{rad} = L_{pp}$$

$$\implies \frac{M^{5.5}}{R^{0.5}} \propto \frac{M^{6.5}}{R^{7.5}}$$

$$\implies R \propto M^{1/7}$$

$$\implies T_c \propto \frac{M}{R} \propto M^{6/7} \implies L \propto M^{5.4}$$

Thus, we get the following scaling relations:

$$R = R_0 (M/M_\odot)^{1/7}$$

$$T_c = 1.5 \times 10^7 \text{ K } (M/M_\odot)^{6/7}$$

$$L \propto L_\odot (M/M_\odot)^{5.4}$$

8.2.2 High Mass Stars on the MS:

Let's now look at the scaling relations for high-mass stars on the MS. Assume the star is:

- Gas pressure supported
- Energy transport = radiative diffusion with e^- scattering
- Fusion = *CNO* cycle

$$L_{rad} \propto M^3$$

$$L_{pp} \propto M \epsilon_{CNO} \propto M \rho T^{20} \propto M^2 R^{-3} \cdot M^{20} R^{-20} \propto M^{22} R^{-23}$$

But:

$$L_{rad} = L_{CNO}$$

$$\implies M^3 \propto \frac{M^{22}}{R^{23}}$$

$$\implies R \propto M^{19/23} \propto M^{0.8}$$

$$\implies T_c \propto \frac{M}{R} \propto M^{0.2} \implies L \propto R^2 T_{eff}^4 \propto M^{1.6} T_{eff}^4 \propto L^{1/2} T_{eff}^4$$

$$\implies T_{eff} \propto L^{1/8} \propto M^{3/8}$$

Thus, we get the following scaling relations:

$$R = R_0 (M/M_\odot)^{0.8}$$

$$T_c = 1.5 \times 10^7 \text{ K } (M/M_\odot)^{0.2}$$

$$T_{eff} = 5777 \text{ K } (M/M_\odot)^{3/8}$$

8.2.3 Very Massive Stars on the MS:

Here, our assumption that the star is gas pressure supported breaks down, and radiation pressure becomes important. Very high-mass stars ($M \geq 1.5M_\odot$) also have convective cores, so we must also consider convective energy transfer. Assume the star is:

- Radiation pressure supported
- Energy transport = convective transport
- Fusion = $p - p$ and *CNO* chain?

For radiation pressure-dominated stars, $P_{rad} \propto \frac{M^2}{R^4} \propto T^4$, so

$$T \propto \frac{M^{1/2}}{R}$$

Recall that convection sets in iff $\frac{dS}{dr} < 0$. In other words:

$$\frac{d \ln T}{d \ln P} > \frac{\gamma - 1}{\gamma} = \frac{2}{5} \text{ for } \gamma = \frac{5}{3}$$

Now, recall the radiative/convective critical gradient:

$$\frac{d \ln T}{d \ln P} = \frac{1}{4} \frac{P}{P_{rad}} \frac{L_r}{L_{edd}(r)} = \frac{1}{4} \frac{P}{P_{rad}} \frac{L_r}{L_{edd}(r)} \frac{L_r/L}{M_r/M}$$

So, convection is induced if:

$$\begin{aligned} \frac{P}{P_{rad}} \frac{L_r}{L_{edd}(r)} \frac{L_r/L}{M_r/M} &\geq \frac{8}{5} \\ \implies \frac{M_r}{M} &\leq \frac{L}{L_{edd}(r)} \frac{L_r}{L} \frac{P}{P_{rad}} \end{aligned}$$

Since $\epsilon_{CNO} \propto \rho T^{20}$, luminosity generation occurs in a very small volume (i.e., $L_r/L = 1$ at a small M_r/M). Also, $\frac{P}{P_{rad}} \downarrow$ as $\frac{L}{L_{edd}(r)} \uparrow$, so $\frac{L}{L_{edd}(r)} \cdot \frac{P}{P_{rad}} \approx 1$. Thus, convection sets in at approx:

$$\frac{M_r}{M} \leq \frac{5}{8}$$

Stars remain on the MS as they burn hydrogen. τ_{MS} is:

$$\tau_{MS} \approx \frac{E_{fusion}}{L} \approx 10^{10} \text{ yr} \left(\frac{M}{M_{\odot}} \right)^{-2}$$

where $L \propto M^3$ and $\epsilon_{fusion} \approx N_p \cdot \Delta E \approx 0.1 \frac{M}{m_p} \cdot \frac{27}{4} \text{ MeV}$. For He and heavier, fusion timescale decreases because the binding energy per particle difference decreases.

8.3 Minimum and Maximum Stellar Mass:

Today, ($z = 0$), stars don't exist with masses $M \leq 0.08M_{\odot}$ or $M \geq 100 - 200M_{\odot}$.

8.3.1 Minimum Stellar Masses:

Minimum mass has to do with the effects of electron degeneracy pressure. Quantum statistics of free particles is important when $\lambda = h/\rho_{thermal} \geq n^{-1/3}$. Thus,

$$n \geq \frac{\rho_{thermal}^3}{h^3} \approx \left(\frac{mk_B T}{h^2} \right)^{3/2}$$

The quantum density of electrons is:

$$n_Q = \left(\frac{2\pi m_e k_B T}{h^2} \right)^{3/2} \approx 10^{26} T_7^{3/2} \text{ cm}^{-3}$$

Thus, if $n_e \geq n_Q$, quantum mechanics becomes important. Recall that at the center of the Sun,

ρ_c	150 g/cm ³
n_e	10^{26} g/cm ³
n_Q	$\approx n_e$

For very low masses, $R \approx M^{3/4} \rightarrow \rho \propto n \propto \frac{M}{R^3} \uparrow$ for $M \downarrow$, and $T \downarrow \rightarrow n_Q \downarrow$. It thus becomes easier to become electron degenerate for decreasing mass. For stars like this, pressure has an electron and ion component:

$$P = P_{e^-} + P_i = \frac{h^2}{5m_e} \left(\frac{3}{8\pi} \right)^{2/3} n_e^{5/3} + \frac{\rho k_B T}{\mu_i m_p}$$

Low-mass stars ($M \leq 0.3M_\odot$) are fully convective $n = 3/2$ polytropes, for which

$$\begin{aligned} P_c &\approx 0.5GM^{2/3}\rho_c^{4/3} \\ \implies \frac{1}{2}GM^{2/3}\rho_c^{4/3} &= \frac{h^2}{5m_e} \left(\frac{3}{8\pi} \right)^{2/3} \left(\frac{\rho_c k_B T}{\mu_i m_p} \right)^{5/3} + \frac{\rho_c k_B T}{\mu_i m_p} \\ \implies T_c &\approx 6.4 \times 10^6 \text{ K} \left(\frac{M}{M_\odot} \right)^{2/3} \rho_c^{1/3} - 1.2 \times 10^5 \text{ K} \rho_c^{2/3} \end{aligned}$$

At low ρ_c , gas pressure dominates and $T_c \uparrow$ with $\rho_c \uparrow$. But at some point T_{max} this reverses until $T_c = 0$ for some ρ_c . These are cold degenerate objects in hydrostatic equilibrium (i.e. brown dwarfs, where $R \propto M^{-1/3}$).

T_{max} occurs when $\frac{dT_c}{d\rho_c} = 0 \implies T_{max} \approx 8 \times 10^7 \text{ K} \left(\frac{M}{M_\odot} \right)^{4/3}$. Physically, this means that a star with mass M and central temperature T_c cannot be self-gravitating if $T \geq T_{max}$.

Scenarios:

1. As $R \downarrow$ and $T_c \uparrow$, the object becomes hot enough for H fusion. If $L_{fusion} \approx L_{rad/conv}$, it becomes a MS star.
2. As $R \downarrow$ and $T_c \uparrow$, the object does not become hot enough for H fusion.
 - Instead, ρ_c becomes so high that e^- degeneracy pressure balances gravity.
 - These objects become brown dwarfs.

Now, let's look at this boundary. Given T_c is $L_{fusion} \approx L_{rad/conv}$? For low-mass, fully convective stars:

$$L_{conv} \approx 0.26 \left(\frac{R}{R_\odot} \right)^2 \left(\frac{M}{M_\odot} \right)^{4/7}$$

$$\epsilon_{pp} \approx 5.2 \times 10^5 \text{ erg/s/g} \cdot \frac{\rho e^{-15.7T_7^{-1/3}}}{T_7^{2/3}}$$

This temperature T_c thus is:

$$T_c \approx 2 \times 10^6$$

K. Thus, for $T \geq 2 \times 10^6$ K, we get an MS star. For $T \leq 10^6$ K, we get a brown dwarf. This boundary corresponds to $M = 0.06M_\odot$.

You can distinguish brown dwarfs and giant planets by looking to see if they've burned their deuterium ^2H or lithium. Brown dwarfs ($M \geq 10M_J$) have burned these, while giant planets do not get hot enough to. Brown dwarf sizes:

$$R_{bd} \propto M^{-1/3}$$

$$R_{bd} \approx 0.04R_\odot \left(\frac{M}{M_\odot}\right)^{-1/3}$$

As $M \downarrow$, $R \uparrow$. The $R \propto M^{-1/3}$ law breaks down at low masses and switches to $R \propto M^{1/3}$ for planets.

8.3.2 Maximum Stellar Masses:

Stars are formed with a mass distribution (Initial Mass Function, or IMF).

$$\frac{dN}{dM} \propto M^{-\alpha}$$

For $M \geq 0.5M_\odot$, $\alpha \approx 2.35$.

$$M_{tot} = \int \frac{dN}{dM} M dM \rightarrow \text{dominated by lower mass stars}$$

$$L_{tot} = \int \frac{dN}{dM} L(M) dM \rightarrow \text{dominated by higher mass stars}$$

since $L(M) \sim M^{3.5}$

Is there an M_{max} ? What would physically cause this? Stellar physics suggests that $M_{max} \sim 100 - 300M_\odot$ at $Z = 0.3 - 1Z_\odot$.

Star formation models suggest $M \geq M_{max}$ stars are unstable and cannot always form. It's possible that high luminosities blow away material needed to form. Most likely explanation is *radiative instability*, though.

IMF

Observations tend to converge on the same result for the IMF of stars larger than $\sim 1M_\odot$. For these stars, $\Phi(M) \propto M^{-2.35}$, or equivalently $\epsilon(M) \propto M^{-1.35}$. Here, ϵ is the number of stars per logarithm in mass equal numbers of stars in intervals that cover an equal

range in logarithm, so there would be the same number from $0.1 - 1M_{\odot}$, from $1 - 10M_{\odot}$, from $10 - 100M_{\odot}$, etc.

This value of $-2.35 / -1.35$ for the exponent is known as the Salpeter slope, after Edwin Salpeter, who first obtained the result. This result means that massive stars are rare both by number and by mass, since Φ and ϵ are strongly declining functions of M .

Mass-Luminosity Relation

The drastic changes seen in the massluminosity relation with mass are primarily due to the **different opacity sources** at work.

1. High mass stars:
 - High $T_c \rightarrow$ fully ionized atoms
 - Scattering of x-rays from free e^- dominates the opacity, with *no temperature dependence*
 2. Mid mass stars:
 - Atoms are only partially ionized \implies strong T dependence in the number of ions n_i .
 3. Low mass stars:
 - Very cool temperatures \implies H_2 (molecular hydrogen) forms, removing the dominant opacity source for solar-type stars.
-

9 Stellar Atmospheres and Spectra:

To first approximation, stars are blackbodies with $T_{eff} = 5800 \text{ K} \left(\frac{M}{M_{\odot}}\right)^{3/8}$. The emission we see from stars comes from the photosphere, which corresponds to the region where the mean free path of light is approximately equal to the pressure scale height.

$$\begin{aligned}
 l &\approx H \\
 \implies \frac{1}{\rho\kappa} &= \frac{P}{\rho g} \\
 \implies P &\approx \frac{g}{\kappa} \\
 \implies n &\approx \frac{g}{k_B T_{eff} \kappa}
 \end{aligned}$$

In the Sun's atmosphere, $n \approx 10^{17} \text{ cm}^3$, $\rho \approx 10^{-7} \text{ g/cm}^3$, $P \approx 0.1 \text{ atm}$. Stellar atmospheres are roughly in thermal equilibrium, which means:

$$N_i \propto g e^{-E_i/k_B T}$$

9.1 The Saha Equation

The Saha Equation is used to determine the number densities of species in systems that are in thermodynamic equilibrium, which is possible because of the known relation of chemical potentials in these types of systems.

Recall the Fermi-Dirac and Bose-Einstein distributions (+ and -):

$$n(p) = \frac{g}{h^3} \frac{1}{e^{(E_p - \mu)/k_B T} \pm 1}$$

where $E_p^2 = \rho^2 c^2 + m^2 c^4$ and $\mu = \left(\frac{\partial E}{\partial N}\right)_{S,V}$. Also note that $n = \int d^3 \rho \cdot n(\rho)$. For $T = 0$ fermions, $\mu = E_F$, where E_F is the Fermi energy.

Classically, $\lambda \ll n^{-1/3}$. In this case, we can assume $e^{(E_p - \mu)/k_B T} \gg 1$

$$\implies n(p) = \frac{g}{h^3} e^{(E_p - \mu)/k_B T}$$

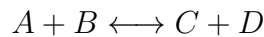
If we set $E_p = mc^2 + \frac{p^2}{2m}$, we get:

$$\begin{aligned} n &= \int d^3 \rho \cdot n(p) = \frac{4\pi g}{h^3} e^{(\mu - mc^2)/k_B T} \times \int d\rho \cdot \rho^2 \cdot e^{-\rho^2/2mk_B T} \\ &= g \left(\frac{2\pi m k_B T}{h^2} \right)^{3/2} e^{(\mu - mc^2)/k_B T} \\ &= g n_Q e^{(\mu - mc^2)/k_B T} \end{aligned} \quad (9)$$

Thus, the classical limit is $n \ll n_Q$, $\lambda \ll n^{-1/3}$, and $e^{(\mu - mc^2)/k_B T} \ll 1$. Thus, the chemical potential for a non-relativistic chemical gas is:

$$\mu = mc^2 - k_B T \ln \left(\frac{n_Q}{n} \right)$$

Now, imagine a system consisting of particles of type A , B , C , and D such that:



Thermodynamic equilibrium is reached when:

$$\mu(A) + \mu(B) = \mu(C) + \mu(D)$$

Note: we couldn't do this for fusion because those reactions are not in thermal equilibrium (it only goes one way). You only get statistical thermal equilibrium with Iron/Nickel, at which point the core is hot enough for photodisintegration to take place.

Consider the following example:



$$\rightarrow \mu(e^-) + \mu(p) \longleftrightarrow \mu(H) + \mu(\gamma)$$

Now, list their chemical potentials:

$$\mu(e^-) = m_e c^2 - k_B T \ln \left(g_e \frac{n_{Q,e}}{n_e} \right)$$

$$\mu(p) = m_p c^2 - k_B T \ln \left(g_p \frac{n_{Q,p}}{n_p} \right)$$

$$\mu(H) = m_H c^2 - k_B T \ln \left(g_H \frac{n_{Q,H}}{n_H} \right)$$

$$\mu(\gamma) = 0$$

Also note that $m_H c^2 = m_p c^2 + m_e c^2 - X$, where $X = 13.6$ eV for ground state H . This gives:

$$\begin{aligned} \frac{-X}{k_B T} - \ln \left(g_H \frac{n_{Q,H}}{n_H} \right) &= -\ln \left(g_p \frac{n_{Q,p}}{n_p} \right) - \ln \left(g_e \frac{n_{Q,e}}{n_e} \right) \\ \Rightarrow \frac{X}{k_B T} &= \ln \left(\frac{g_H n_{Q,H} n_p n_e}{n_H g_p g_e n_{Q,p} n_{Q,e}} \right) \\ \Rightarrow \boxed{\frac{n_p n_e}{n_H} &= \frac{g_p g_e}{g_H} \cdot n_{Q,e} e^{-X/k_B T}} \end{aligned}$$

This is the Saha equation.

9.1.1 Pure H gas:

At what temperatures is H gas half ionized? Let $n_H = n_e + n_p$, and $g_H = 2$, $g_p = 1$, $g_e = 2$. Then

$$n_H = \left(\frac{2\pi m_e k_B T}{h^2} \right)^{3/2} e^{-X/k_B T}$$

If $n = 10^7 \text{ cm}^{-3}$, we get $T = 1.5 \times 10^4$ K. Since $k_B T = X$ when $T = 1.5 \times 10^5$ K, we get half ionization when $k_B T \approx 0.1 X_{ion}$. This is a general relationship:

He and Ne	$X_{ion} \approx 25$ eV	$T_{ion} \approx 30,000$ K
H, C, N, O	$X_{ion} \approx 10$ eV	$T_{ion} \approx 10,000$ K
Ca, K, Mg, Na	$X_{ion} \approx 5$ eV	$T_{ion} \approx 5,000$ K

For hydrogen, transition lines in optical are Balmer lines ($n' = 2$) (we don't see Lyman emission ($n' = 1$) because it requires IR and the Sun's spectrum peaks in the visible). We can find $n_{n=2}/n_{tot}$ as a function of T . There is a strong dropoff at high and low temperatures, because all electrons are in $n = 1$ state.

There's an important dimensionless number: $n_{n=2}/n_{tot} \geq 10^{-8}$ for there to be different random walks out of the system and for transitions to be visible.

Last, remember that absorption lines are due to temperature gradients in stellar photospheres. Consider frequencies ν_1 and ν_2 such that $\sigma_{\nu, 1} > \sigma_{\nu, 2}$. Since we see photons from where $l_\nu = H = \frac{1}{n\sigma_\nu}$, $l_{\nu, 2} > l_{\nu, 1}$. Since T_ν increases for larger l_ν (deeper into the star), $T_{\nu, 2} > T_{\nu, 1}$. As a result, ν_2 has a higher F_ν than ν_1 . This creates dips in the spectrum.

10 Stellar Evolution:

10.1 Post-Main Sequence Evolution:

As we have emphasised before, the details of the ways stars evolve off the main sequence and their ultimate fate all depend on the stellar mass. In this section, we consider low mass stars, with $M \sim 1M_\odot$.

10.1.1 The Red Giant Branch (RGB):

Let's begin at the end of the main sequence evolution, where the star is burning H in a shell encompassing an isothermal He core. Because of the mirror action of the shell, the outer layers expand and cool and the star moves to the right in the H-R diagram. During this phase, which for a $1M_\odot$ lasts ~ 2 Gyr, the star moves along the "subgiant branch" (SGB). At the end of this stage, the He core becomes degenerate.

As the star expands, however, the effective temperature cannot continue to fall indefinitely. With the expansion of the stellar envelope and the decrease in effective temperature, the photospheric opacity increases due to the additional contribution from H- ions. When the temperature of the outer layers of the star falls below $\sim 5000 \equiv 5 \times 10^3$ K, they become fully convective. This enables a greater luminosity to be carried by the outer layers and hence abruptly forces the evolutionary track to travel almost vertically upwards to the red giant branch (RGB).

envelope expands $\rightarrow \downarrow T_{eff} \rightarrow \downarrow \kappa_{photosphere}$
 when $T_{eff} \leq 5 \times 10^3$ K, \rightarrow fully convective outer layers
 \implies greater $L_{outer} \rightarrow$ forces evolutionary track to travel vertically upwards to the RGB

The star now moves along the same path, but in reverse, followed by a *fully convective pre-main-sequence star* on its approach to the main sequence, which is a nearly vertical line in the H-R diagram known as the Hayashi track.

- **Hayashi Track** \rightarrow the region to the right is forbidden; there's no mechanism that can transport the luminosity out of the star at such a low T_{eff}

A $1M_\odot$ star will spend 0.5 Gyr on the RGB to the He flash at an accelerating evolutionary pace, driven by what is occurring in the core.

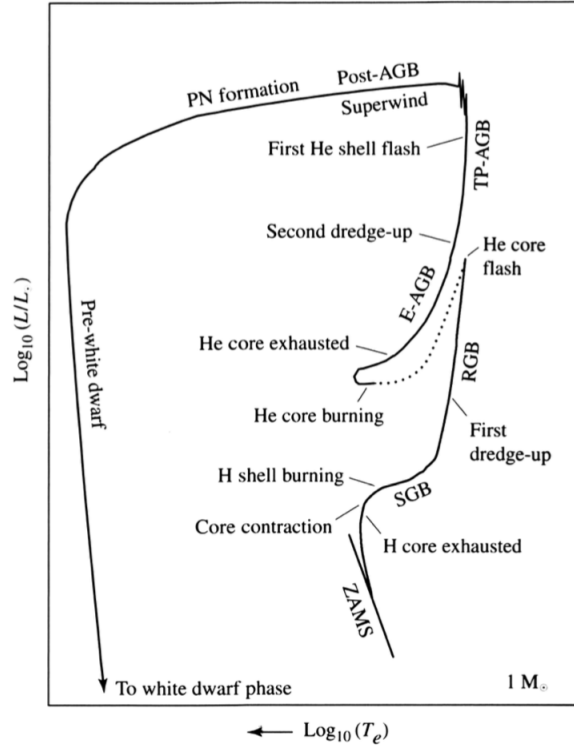


Figure 3: Schematic diagrams of the evolution of a $1M_{\odot}$ star of solar metallicity, from the main sequence to a white dwarf.

- As H-fusion in the shell deposits more He onto the core, the mass of the core increases.
- For a fully degenerate gas \rightarrow increased mass makes core contract
- Core contracts $\rightarrow \rho_{shell, H}$ increases
- $\uparrow \rho_{shell, H} \rightarrow \uparrow$ fusion efficiency $\rightarrow \uparrow L$
 - This is a runaway process
- By the end of the RGB, the degenerate He core reaches a mass of $\sim 0.5M_{\odot}$ and has contracted enough to achieve the temperature required to ignite He fusion

For a star with a degenerate core, the density contrast between the core and the envelope is so large that the two are practically decoupled. The pressure at the bottom of the extended envelope is very small compared to the pressure at the edge of the core and in the H-burning shell separating core and envelope.

efficiency of the shell burning $\equiv M_{He\ core}$ (NOT by the envelope)

$\Rightarrow M_{He\ core} \propto L_{RG} \equiv$ hydrogen shell-burning source

$$L \approx 2.3 \times 10^5 \left(\frac{M_c}{M_{\odot}} \right)^6 L_{\odot}$$

Thus, the evolutionary tracks of stars of different masses all converge onto the Hayashi line that is the RGB; from the position of a star on the RGB we can deduce the value of M_c , but the total mass is more difficult.

10.1.2 Metallicity Dependence of the RGB:

The red giant branch does however exhibit *a metallicity dependence*. As we discussed in earlier lectures, **fully convective stars are on the Hayashi line** which is the locus of the lowest values of T_{eff} at which a star of a given luminosity can shine. Convection is related to the opacity, and the opacities of stellar atmospheres depend on metallicity. This is the case even when H is the main source of opacity because the metals provide the free electrons that form H.

Convection

An increase in opacity κ in a stellar atmosphere will lead to a larger temperature gradient dT/dr (if the luminosity stays the same). This is from the Eddington equation for thermal equilibrium:

$$\frac{dT}{dr} = \frac{-3}{4} \cdot \frac{1}{ac} \cdot \frac{\kappa\rho}{T^3} \cdot \frac{L_r}{4\pi r^2}$$

where a is the radiation constant, $a = 4\sigma/c$, σ is Stefan-Boltzmann constant, κ is the opacity and the other symbols have their usual meanings. As the temperature decreases from $T \sim 10^7$ K, the opacity rises steeply with a Kramers law $\kappa \propto T^{-3.5}$. Thus, as we move from the core to the outer regions within a stellar interior, the temperature gradient is expected to become increasingly steep. A very steep temperature gradient is unstable, whether in a star or the Earth's atmosphere.

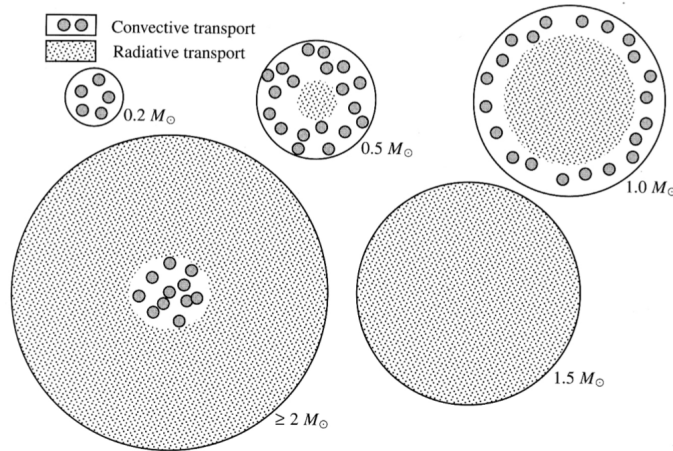
Which Stars are Convective?

From the above equation, we see that the temperature gradient is proportional to the opacity κ ; thus, we expect that in layers where the opacity is very high, the temperature gradient required for radiative energy transport becomes unachievably steep. We also know that stellar opacities increase dramatically as T decreases from 10^6 to 10^5 K; at $T \sim 10^5$ K the gas is only partly ionised (at typical stellar densities); the rise in κ is produced by the availability of many bound-bound and bound-free transitions.

Hand in hand with this is the increase in the specific heats, and therefore the increase in γ as the gas becomes partly, as opposed to fully, ionised. As we have discussed, this will increase the adiabatic $|d \ln P / d \ln T|$ gradient, leading to convection.

- For both reasons, **convection will occur in the outer layers of cool stars.**
- In a G0 V star the convective layer is thin, while main sequence M stars are almost fully convective.

- Red giants and supergiants are also convective over most of their interiors.
- Convection is also important in stellar layers where the ratio $L/4\pi r^2$ is high (see above equation), that is where large luminosities are generated over small volumes. This is the situation in the cores of massive stars, given the steep temperature dependencies of the CNO cycle and the triple-alpha process



The above figure shows the following: Zones of convection and radiation in main-sequence stars of various masses. The lowest mass stars are completely convective. A radiative core develops at $M \approx 0.4M_{\odot}$, and a star is fully radiative at $M \approx 1.5M_{\odot}$. The core region is again convective for masses $M \geq 2.0M_{\odot}$. The relative sizes of the stars shown here are approximately correct, while on the main sequence.

With a higher metallicity, an optical depth $\tau \approx 2/3$ is reached sooner, or at lower density, as we travel from the stellar "surface" to the core (recall $\tau \approx 2/3$ is approx the photosphere). Thus, metal-rich stars of a given mass have slightly larger radii and lower effective temperatures than stars of the same mass but lower metallicity. For the same reason, the RGB of metal-rich stars runs at slightly lower temperatures than that of metal-poor stars. A vivid demonstration is provided by the colour-magnitude diagrams of stellar systems consisting of multiple populations:

$$\boxed{\uparrow \text{metallicity} \rightarrow \uparrow R \text{ and } \downarrow T_{eff}}$$

$$\boxed{\Rightarrow \text{RGB runs at slightly lower temperatures than metal-poor stars}}$$

The very steep temperature dependence of the opacity at the effective temperatures of red giants, $\kappa \propto T^9$, provides an intuitive explanation for the fact that the Hayashi line is close to vertical on a $L - T_{eff}$ diagram. Suppose that a cool star of constant L could increase its radius, even by a small amount. This would lower the value of T_{eff} and therefore the opacity κ of the outer layers. As a result, we would be able to see deeper into the star, down to a depth where $\tau \approx 2/3$, at nearly constant T_{eff} .

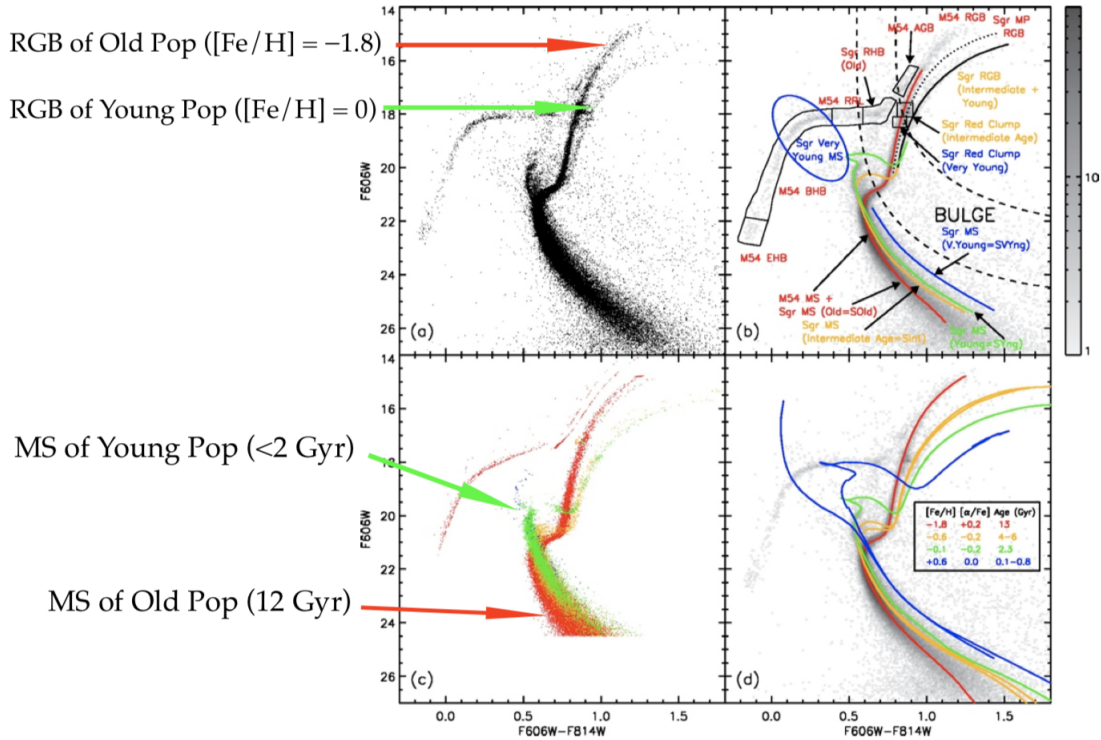


Figure 4: Colour-magnitude diagram (CMD) of 60,000 stars in the field of the globular cluster M54, which also includes the dwarf spheroidal galaxy Sagittarius (Sgr), which is in the process of merging with our own Galaxy. Multiple populations, of different ages and metallicities, can be distinguished in this complex CMD, allowing the past history of star formation of this companion galaxy to the Milky Way to be reconstructed. Highlighted in panel (a) are two well-separated red giant branches, whose metallicities differ by two orders of magnitude.

10.1.3 Mass Loss on the RGB:

As the stellar luminosity and radius increase while a star evolves along the giant branch, the envelope becomes loosely bound and it is relatively easy for the large photon flux to remove mass from the stellar surface via radiation pressure on atoms and grains.

Grains are microscopic solid particles that can condense out of the gas phase at the values of temperature and pressure typical of the extended atmospheres of late-type giant and supergiant stars. Their presence in these environments is indicated by a number of infrared spectral features, such as the $9.7\mu\text{m}$ band due to silicates, which can appear in emission or absorption in the spectra of red giants and supergiants. The winds from these stars are responsible for distributing grains into the interstellar medium, where they can subsequently grow through accretion of atoms. Interstellar grains, or dust as they are often referred to, are an important constituent of the diffuse interstellar medium. They regulate the heating and cooling of the ISM, act as a catalyst in the formation of H_2 molecules, and of course are responsible for interstellar extinction, the process that reddens the light of all stars.

Returning to mass loss on the RGB, red giant stars are observed to lose mass in the form of a slow wind ($v_{wind} \approx 5 - 30 \text{ kms}^{-1}$) at a rate $\dot{M} \approx 10^{-8} M_{\odot} \text{ yr}^{-1}$. A $1M_{\odot}$ star loses $\sim 0.3M_{\odot}$ of its envelope mass by the time it reaches the tip of the giant branch. When calculating the effect of mass loss in evolution models an empirical formula due to Reimers is often used:

$$\dot{M} = -4 \times 10^{-13} \eta \frac{L}{L_{\odot}} \frac{R}{R_{\odot}} \frac{M_{\odot}}{M} M_{\odot} \text{ yr}^{-1}$$

where the efficiency factor $\eta \approx 0.25 - 0.5$. However, this relation is based on observations of only a handful of stars with well-determined stellar parameters. Note that this implies that a fixed fraction of the stellar luminosity is used to lift the wind material out of the gravitational potential well of the star.

10.1.4 The First Dredge-up:

As the star climbs up the RGB, its convection zone deepens until the base reaches down into regions where the chemical composition has been modified by nuclear processes. This transports processed material from the deep interior to the surface in what is referred to as the first dredge-up phase. This phase provides us with the first opportunity to verify empirically our ideas about nuclear burning which, up to this point, has been completely hidden from view.

For example, Li is destroyed by collisions with protons at relatively low temperatures, $T \rightarrow 2.7 \times 10^6 \text{ K}$; as a consequence of the first dredge-up *the atmospheres of evolved stars exhibit a Li deficiency* compared to the Li abundance of the proto-stellar nebula. Indeed, **the Li abundance is often used as a test to decide whether the atmospheric abundances can be trusted to represent the composition** of the gas from which the star formed.

Similarly, the surface He abundance increases and the H abundance decreases while a star ascends the RGB. In intermediate mass stars ($M \approx 5M_{\odot}$), the convective envelope brings material processed by the CNO cycle to the surface. The C-N cycle reaches equilibrium before the O-N cycle, and thus CN-processed material (N enriched, C depleted) is first exposed on the surface. The N abundance increases by a factor of ~ 2 , C is decreased by 30% and O is unchanged. Many red giants are observed to have CN-processed material in their atmospheres.

10.1.5 The Red Giant Tip and the Helium Flash:

At the tip of the RGB, the central temperature and density have finally become high enough ($T > 10^8$ K) for quantum tunnelling to overcome the Coulomb barrier between He nuclei, **allowing the triple-alpha process** to begin. Some of the resulting ^{12}C is further processed into ^{16}O via capture of an alpha particle. This is the onset of the helium burning phase of evolution. Unlike H-burning, the reactions involved in He-burning are the same for all stellar masses. However, the conditions in the core at the ignition of helium are very different in low-mass stars (which have degenerate cores) from stars of higher mass (with non-degenerate cores).

- Low mass stars ($1M_{\odot}$)
 - Electrons in the core are completely degenerate by the time the star reaches the tip of the RGB.
 - Ignition in a degenerate core results in an explosive start of the fusion known as the Helium Flash.
 - Ignition of He-fusion raises the temperature of the core, but this does not raise the pressure, because in a degenerate gas $P \neq f(T)$
 - Thus, as T increases the core does not expand, and the density remains the same. The energy generation rate of the triple alpha reaction has an extraordinarily steep dependence on T ($\varepsilon_{3\alpha} \propto Y^3 \rho^2 T^{40} \implies$ rise in T leads to more efficient fusion, which in turn raises the $T \implies$ a degenerate core is ignited acts like a bomb
 - Thermonuclear runaway leads to an enormous overproduction of energy: at maximum, the local luminosity in the helium core is $L_c \sim 10^{10}L_{\odot}$, comparable to the luminosity of a small galaxy! ($\tau \sim$ several seconds).
 - * All the nuclear energy released is absorbed by expansion of the non-degenerate layers surrounding the core, so none of this luminosity reaches the surface.
 - * The short duration τ , and the presence of a very extended convective envelope that can absorb the energy created by the flash explain why the He flash has never been observed, other than in our computers.

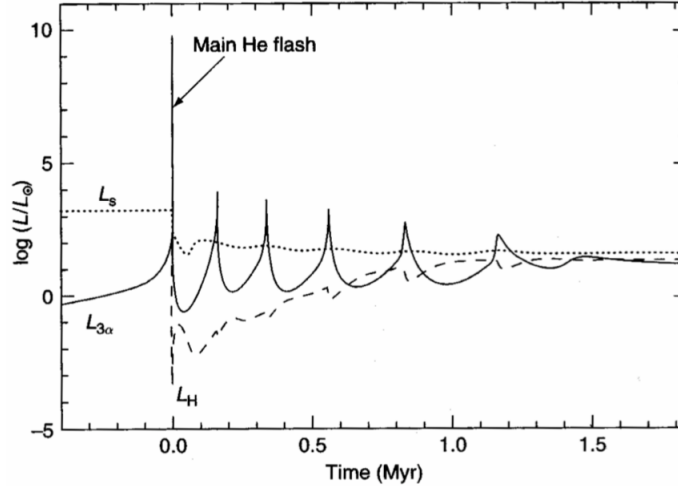


Figure 5: The helium flash. Evolution with time of the surface luminosity (L_s), the He-burning luminosity ($L_{3\alpha}$) and the H-burning luminosity (L_H) during the onset of He burning at the tip of the RGB in a low-mass star. Time $t = 0$ corresponds to the start of the main helium flash.

- * Since the temperature increases at almost constant density, degeneracy is eventually lifted when $T_c \approx 3 \times 10^8 \text{K}$. Further energy release increases the pressure when the gas starts behaving like an ideal gas and thus causes expansion and cooling.
- * Results in \downarrow energy generation rate until it balances the energy loss rate and the core settles in thermal equilibrium at $T_c \approx 10^8 \text{ K}$.
- * Further nuclear burning is thermally stable.
- After the He flash, the whole core expands somewhat but remains partially degenerate. In detailed models, a series of smaller flashes follows the main He flash for $\sim 1.5 \text{ Myr}$, before degeneracy in the centre is completely lifted and further He burning proceeds stably in a convective core.
- This is the situation when stars with a non-degenerate core reach $T_c \sim 10^8 \text{ K}$ at the tip of the RGB.
 - * $\uparrow T_c \implies \uparrow P$
 - * Core expands $\rightarrow T_c \downarrow$ and $P \downarrow \implies$ energy production drops and $R_{core} \downarrow$ until it reaches hydrostatic equilibrium again
 - * Gravity acts like a regulator and the star does NOT experience a HE flash

The dividing line between stars with degenerate and non-degenerate cores at the tip of the RGB is $\sim 2M_\odot$; stars with $M \leq 2M_\odot$ undergo a He flash, while in those with $M \geq 2M_\odot$ He burning is ignited without a thermonuclear runaway event.

So, in this case, gravity acts like a regulator and the star does not experience a He flash.

10.1.6 The Horizontal Branch

The evolution of the star is resumed at point G when the star has settled into a new equilibrium configuration with an expanded non-degenerate core which is hot enough to burn He. The star now has 2 sources of energy generation:

1. Core He fusion
2. Shell H fusion
 - H-burning shell has also expanded and now has lower T and $\rho \implies$ generates less energy than when star was at the upper end of the RGB
 - Lower L_{tot} is insufficient to keep the star in this distended red giant phase $\implies R \downarrow$ and $L \downarrow$ (star shrinks and dims) and settles on the horizontal branch
 - L and R have decreased by more than 1 order of magnitude from their values just before the He flash
 - Core has expanded (from a degenerate to a non-degenerate state)
 - Envelope has simultaneously contracted, with the H-burning shell acting as a mirror
 - The horizontal branch is the core He-burning equivalent of the core H-burning main sequence
 - $1M_{\odot}$ star spends $\tau \sim 1 \times 10^{10}$ yrs on the main sequence
 - $1M_{\odot}$ star spends ~ 120 Myr, or 1% of its main sequence lifetime on the HB branch because of the much higher luminosity of the He-burning phase

10.1.7 The Horizontal Branch Morphology

The location of the star in the H-R diagram does not change very much while on the horizontal branch, always staying close to (but somewhat to the left of) the RGB. Its luminosity is $\sim 50 : L_{\odot}$ for most of the time, a value determined mainly by the core mass. Since the core mass at the start of helium burning is $\sim 0.45M_{\odot}$ for all low-mass stars, irrespective of stellar mass, **the luminosity at which He burning occurs is also almost independent of the total stellar mass.** Thus, **it is only the envelope mass that varies from star to star, either because of differences in mass on the ZAMS, or as a result of different amounts of mass loss on the RGB.**

- Solar metallicity– all core He-burning stars occupy a similar locus in the H-R diagram, which is referred to as the ‘red clump’.
 - May be the red extreme of the HB

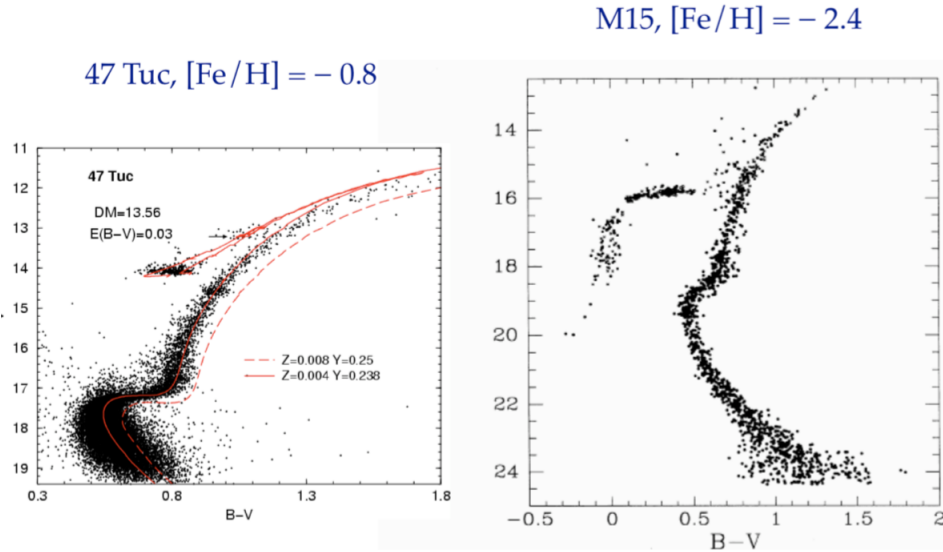


Figure 6: The Fe abundances of the stars in these two Galactic globular clusters differ by a factor of ~ 40 . In the more metal-poor globular cluster, M15 on the right, the horizontal branch extends much further to the blue (hotter effective temperatures, implying smaller radii) than in the more metal-rich one (47 Tuc, on the left).

- Metal-poor globular clusters– stars are found to be spread out over a range of effective temperatures at the same approximate luminosityhence the ‘horizontal branch’ nomenclature.
 - Location of a star on the HB is a reflection of its envelope mass: stars with smaller envelopes (and hence radii) are bluer (and are therefore found on the left of the HB).
 - The extent of the horizontal branch in globular clusters seems to be related to their metallicity.
- Metal-rich globular clusters– tend to have a red HB

Metallicity may not be the only factor at play here: let’s invoke a second parameter. Age, He content, and rotation have been proposed, but the underlying cause of different HB morphologies remains a long-standing problem in stellar astrophysics.

Once a star has entered the HB (on the left, the right or in between), evolution moves it to the right during the core He fusion phase, due to the increasing depth of the convection zone.

10.1.8 The Asymptotic Giant Branch (AGB):

At this point, the star has exhausted its supply of He in the core which now consists of C and O. The core contracts again:

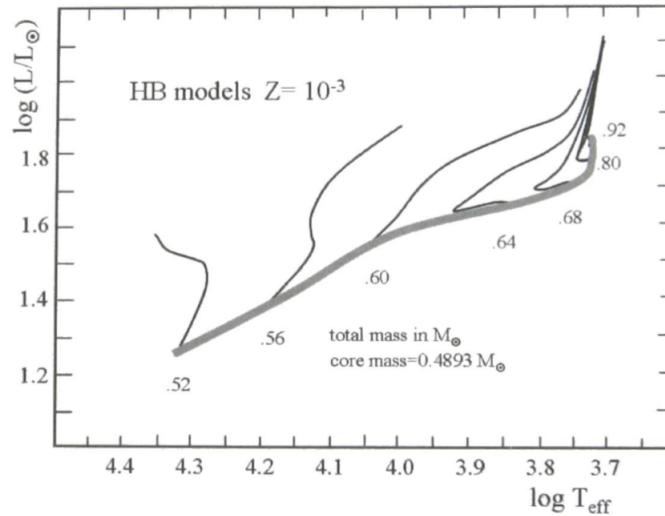


Figure 7: Location of the zero-age horizontal branch (thick grey line) for a metallicity $Z = 0.001$ which is typical of Galactic globular clusters. The models shown all have the same core mass ($M_c = 0.489M_\odot$) but varying total (i.e. envelope) mass, which determines their position in the H-R diagram. Evolution tracks during the HB phase for several total mass values are shown as thin solid lines.

1. $M < 8M_\odot$ stars

- Insufficient gravitational energy to generate the high temperatures required to fuse C and O into heavier nuclei. Thus, no more core fusion takes place in these stars.
- Core contraction generates sufficient heat for the surrounding layer of He to start fusing in a shell.
- Contracting core \rightarrow strong expansion of the star's outer layers, causing $T_{surf} \downarrow$ and moves the star to the right and up in the H-R diagram along the AGB
- A $1M_\odot$ AGB can reach $L \sim 10^5 L_\odot$

The AGB is the shell He-burning analogue of the shell H-burning RGB.

1. Solar metallicities

- AGB close to the RGB

2. Metal-poor globular clusters

- AGB and RGB are well separated

A this point, the star consists of:

1. A degenerate C+O core
2. A He- burning shell

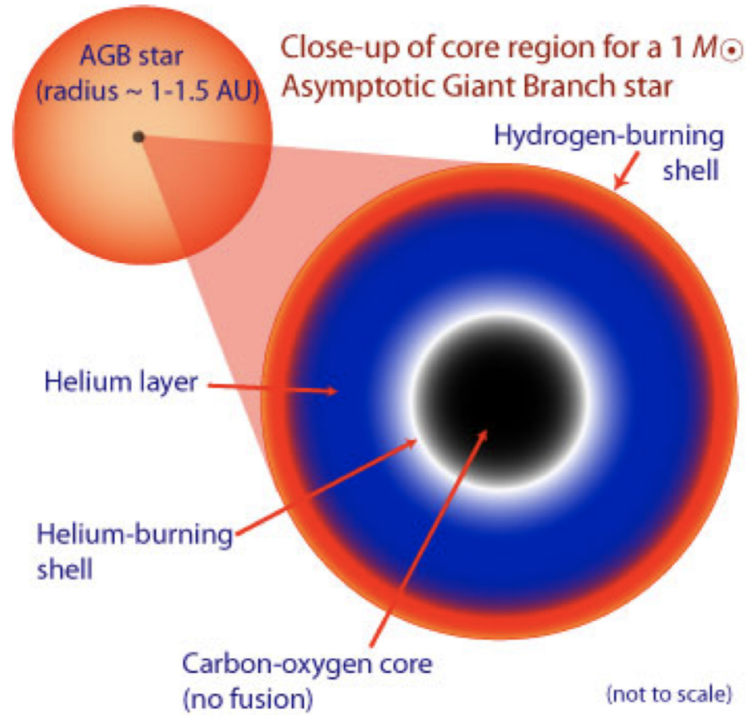


Figure 8: Schematic structure of a solar mass star during the RGB phase.

3. An inert He-shell around it
4. A H-burning shell
5. An outer H-rich convective envelope

The evolution is now complex because the huge differences between the two nuclear fusion processes do not allow a steady state to exist. The two shells supply the luminosity of the AGB star alternately in a cyclical process, or a thermal pulsation, which has a period of $\tau \sim 10^3$ yr, with the changes triggered by shell flashes.

1. $1M_{\odot}$ stars
 - Spend $\sim 5 \times 10^6$ yr on the AGB
 - Expansion and cooling $\rightarrow \kappa \uparrow$ and \uparrow depth of the convection zone, which can reach down to the chemical discontinuity between the H- rich outer layer and the He-rich region between the two burning shells.
 - Mixing that results during this second dredge-up phase increases the He and N content of the envelope
2. Stars $> 2M_{\odot}$
 - There a third dredge-up as the tip of the AGB is approached, driven by thermal pulsations \rightarrow brings to the surface C-rich material and 's-process' elements

- Stars $> 3M_{\odot}$
 - * Base of the convective envelope becomes hot enough for the CN cycle to operate and the dredged-up C is converted to N in a process called ‘hot bottom burning’

At the low temperatures of the atmospheres of AGB stars, most of the C and O atoms are bound into CO molecules, since this is the most stable molecule. In the protostellar nebula, $C/O \sim 0.5$. If this initial abundance has not been changed appreciably and all the C is locked in CO molecules, then the remaining O atoms form oxygen-rich molecules and dust particles, such as TiO, H₂O and silicate grains. The spectra of such O-rich AGB stars are classified as type *M* or *S*. However, as a result of repeated dredge-up events, at some point the C/O ratio can exceed unity. In this case all O is locked into CO molecules and the remaining C forms carbon-rich molecules and dust grains, e.g. C₂, CN, C_nH_n, and carbonaceous grains like graphite and SiC. Such more evolved AGB stars are classified as carbon stars with spectral type *C*. Besides carbon, the surface abundances of many other elements and isotopes change during the Thermal-Pulse (TP) AGB phase.

10.1.9 Slow Neutron Capture Nucleosynthesis:

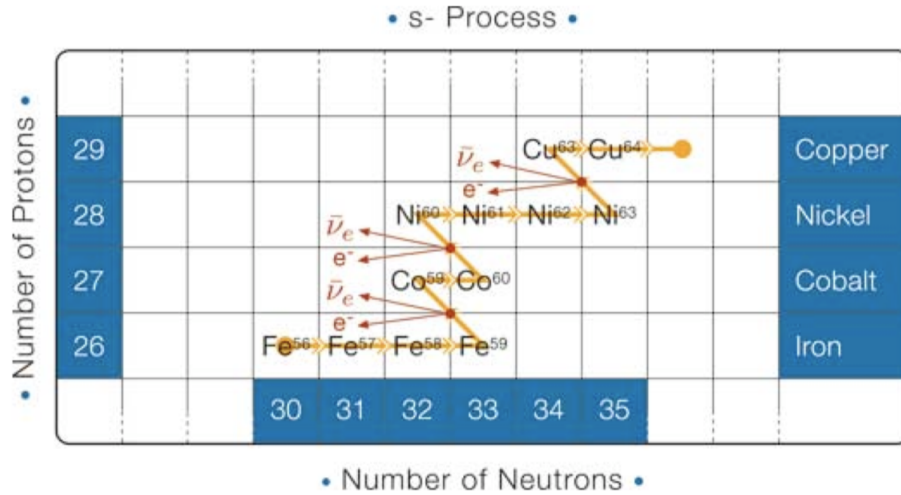
Direct evidence for active nucleosynthesis in AGB stars was provided in 1953 by the detection of technetium (⁴³Tc), the lowest atomic number element without any stable isotopes: every form of it is radioactive. The longest lived isotope, ⁹⁹Tc, decays on a timescale of only 2×10^5 yr.

Neutron Capture

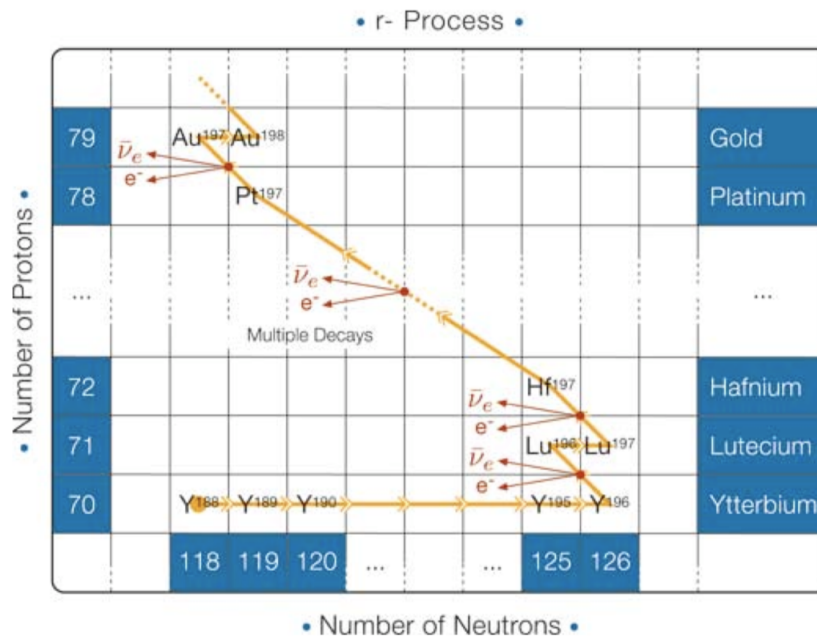
Neutron capture is the mechanism whereby elements heavier than Fe are thought to be produced in stars.

At $T \approx 1.5 \times 10^9$ K, photodisintegration of nuclei becomes important and creates a mixture of neutrons, protons and other nuclei. Neutrons play an important role here. Since *neutrons do not experience a Coulomb barrier*, they can easily penetrate the nuclei of even fully ionized heavy elements, such as Fe^{+26} . If they are captured by the nucleus, new neutron-rich isotopes can be produced. Such isotopes can be either stable or unstable.

It is important to distinguish between slow and rapid neutron capture (termed the s-process and the r-process), depending on the relative timescales of β -decay and neutron capture. In the example of the s-process in Figure 10.1.9, ⁵⁶Fe absorbs a neutron to form ⁵⁷Fe. Subsequent capture of two more neutrons leads to the formation of ⁵⁹Fe. Of the four Fe isotopes shown, the three lighter ones are stable, but ⁵⁹Fe is unstable, with a half-life of 44.5 days. Thus, if the flux of neutrons is not high and the interval between successive n-captures is longer than the half-life of ⁵⁹Fe, there is time for ⁵⁹Fe to decay to ⁵⁹Co by β -decay ($n \rightarrow p + e^- + \nu_e$). The process can continue to form higher and higher mass elements, as shown in Figure 10.1.9.



On the other hand, if the flux of neutrons is sufficiently high and the time interval between subsequent neutron captures is small compared to the half-life of the isotopes concerned, super-neutron-rich isotopes can be formed, as in the example of the r-process shown in Figure 10.1.9. When the neutron flux stops, these super-neutron-rich isotopes will undergo a series of β -decays until a stable isotope is reached.



- r-process
 - Eu
 - Takes place in supernova explosions
- s-process
 - Cu and Pb

- Takes place in AGB stars

Trans-Fe-peak elements can be formed by either s- or r-process nucleosynthesis, or both, depending on the stability of their neighbors in the Periodic Table.

Spectroscopic observations actually show that many AGB stars are enriched in elements heavier than Fe, such as Zr, Y, Sr, Tc, Ba, La and Pb. These elements are produced via slow neutron capture reactions on Fe nuclei, the **s-process**.

In this context slow means that the time between successive neutron captures is long compared to the β -decay timescale of unstable, neutron-rich isotopes. The synthesis of s-process elements requires a source of free neutrons, which can be produced in the He-rich intershell region by a number of reactions. AGB stars are nowadays considered to be major producers in the Universe of carbon, nitrogen and of elements heavier than iron synthesised via the s-process. They also make an important contribution to the production of ^{19}F , ^{25}Mg , ^{26}Mg and other isotopes.

10.1.10 Mass loss and the post-AGB phase:

During the AGB phase, the mass loss increases dramatically from $\dot{M} \approx 10^8$ to $\dot{M} \approx 10^4 M_{\odot} \text{ yr}^{-1}$. We can easily see this:

$$\frac{dM_{star}}{dt} = \frac{-dM_{wind}}{dt}$$

$$\frac{dM_{env}}{dt} = \frac{-dM_{wind}}{dt} - \frac{dM_{core}}{dt}$$

but

$$\frac{dM_{wind}}{dt} = f(L)$$

and

$$L = f(M_{core})$$

In fact, mass loss becomes so strong on the AGB that the entire H-rich envelope can be removed before the core has had time to grow significantly. The lifetime of the TP-AGB phase, $t_{TPAGB} \sim 1 - 2 \times 10^6$ yr, is essentially determined by the mass-loss rate.

The high mass-loss rate distributes the chemical elements and dust grains found in the outer atmospheres of AGB stars into the surrounding interstellar medium. Many AGB stars (known as OH/IR stars) are completely enshrouded in a dusty circumstellar envelope which renders them invisible at optical wavelengths. The mechanisms driving such strong mass loss are not fully understood, but it is likely that both *dynamical pulsations and radiation pressure on dust particles* play a role.

AGB stars undergoing strong radial pulsations are known as ‘Mira variables’. Observationally, a correlation is found between the pulsation period and the mass-loss rate. As a

star evolves towards larger radii along the AGB, the pulsation period increases and so does the mass-loss rate, from $\dot{M} \sim 10^{-8}$ to $\sim 10^{-4} M_{\odot} \text{ yr}^{-1}$ for pulsation periods in excess of about 600 days. This phase of very strong mass loss is sometimes called a *superwind*. Once an AGB star enters this superwind phase, the H-rich envelope is rapidly removed marking the end of the AGB phase. The high mass-loss rate during the superwind phase therefore determines both the maximum luminosity that a star can reach on the AGB, and its final mass, i.e. the mass of the white-dwarf remnant.

The mass loss rate increases until the mass of the remaining envelope has reached some minimum value, $10^{-2} - 10^3 M_{\odot}$, such that a convective envelope can no longer be sustained and the envelope starts to contract into radiative equilibrium and the star leaves the AGB.

- $\downarrow R$ occurs at constant L b/c H-burning shell is still fully active and the star keeps following the core mass-luminosity relation
- Star thus follows a horizontal track in the H-R diagram towards higher T_f (post-AGB phase of evolution).
 - Star remains in complete equilibrium during this phase
 - Evolution towards higher T_{eff} is caused by the decreasing mass of the envelope ($\downarrow M_{envelope}$), which is eroded at the bottom by H-shell burning and at the top by continuing mass loss.
 - $\tau \sim 10^4 \text{ yr}$

10.1.11 Planetary Nebulae:

As the star gets hotter and T_{eff} exceeds 30000 K, two effects come into play: (1) the star develops a weak but fast wind ($\dot{M} \approx 10^6 M_{\odot} \text{ yr}^{-1}$, $v_{exp} \approx 1000 \text{ km s}^{-1}$), driven by radiation pressure in UV absorption lines (similar to the winds of massive OB-type stars); and (2) the strong UV flux destroys the dust grains in the circumstellar envelope, dissociates the molecules and finally ionizes the gas. Part of the circumstellar envelope thus becomes ionized (an HII region) and starts radiating in recombination lines: a young Planetary Nebula (PN) is born. (PNs have nothing to do with planets, of course. The name has its origin in the fact that, like planets, they are not point-like sources, and therefore did not appear to twinkle due to atmospheric turbulence when observed with the naked eye by early astronomers. The misnomer has stuck).

Planetary nebulae result from the interaction between the slow AGB wind ($v \approx 10 - 15 \text{ km s}^{-1}$) and the fast wind from the central star ($v \approx 50 \text{ km s}^{-1}$). The fast wind sweeps up and accelerates the AGB wind, forming a compressed optically thin shell from which the radiation is emitted.

10.1.12 The spectra of planetary nebulae:

10.2 Small Stars:

Let's start at the end of the hydrogen fusion (main sequence) stage. The MS lifetime is

$$\tau_{MS} \approx 10^{10} \text{ yr} \left(\frac{M}{M_{\odot}} \right)^{-2/5}$$

After MS, star is left with a He core with $M \approx 0.1M_{*}$. He fusion does not begin immediately. The core undergoes KH contraction, and the envelope expands. T_c and ρ_c increase until one of the 2 fates is met:

1. The core is supported by electron degeneracy pressure and becomes a white dwarf
 - Requires:
 - $M_c \leq 1.4M_{\odot}$
 - $M_{ZAMS} \leq 8M_{\odot}$
 - $T_{c,max} = 7 \times 10^8 \text{ K}$
 - Fusion usually stops at C/O (sometimes O/Ne).
 - Generally occurs after He fusion
2. Core collapses into neutron star or black hole (sometimes with a supernova)
 - If $M \geq 1.4M_{\odot}$, electron degeneracy pressure cannot support contracting core and heavier elements (up to Fe) begin to fuse
 - Core collapses eventually into NS, BH, or SN
 - $M_{ZAMS} \geq 8M_{\odot}$
 - For $M_{ZAMS} \geq 120M_{\odot} - 150M_{\odot}$:
 - Pair-instability supernovae \rightarrow star explodes completely and fuses heavier elements as it collapses

For He cores, degeneracy pressure isn't very important if $M \geq 2M_{\odot}$. He fusion requires $T \approx 10^8 \text{ K}$. Since $T \propto M/R$, the core radius decreases by a factor of 10.

10.2.1 $M \geq 2M_{\odot}$:

1. On MS:
 - This star has a He core. The He core contracts with a constant temperature (i.e. $dT/dr \approx 0 \rightarrow Fe \approx 0$). Hydrogen shell fusion occurs and supplies the luminosity ($L_{shell} \approx L_{surface}$). This increases the *mass* of the He core. As the core continues to KH contract, T and ρ of H shell increase, increasing L_{shell} . Once $L_{shell} > L_{rad}$,

convection kicks in. The envelope becomes fully convective and the star becomes a red giant, moving up the Hayashi track until He core fusion begins

2. on RGB:

- Star moves up RGB until He fusion begins. It undergoes the "Blue Loop" until it's left with a C/O core

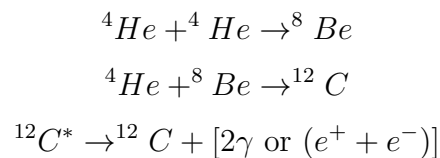
10.2.2 $M \leq 2M_{\odot}$:

The star has a He core. This core becomes degeneracy pressure supported. In the core, $R \propto M^{-1/3}$, so $T_{shell} \propto \frac{M}{R} \propto M^{4/3}$. H shell fusion increases the mass of the core, so T_{shell} and L_{shell} increase. The star becomes a red giant until T_{core} increases enough for He fusion to begin.

- This does NOT begin if $M_{*} \leq 0.5M_{\odot}$
 - Never begins He fusion → left with He degenerate cores.
 - Binary stripping leaves a He white dwarf
- $0.5M_{\odot} - 2.0M_{\odot}$ stars with degenerate He cores: undergo H shell fusion until the core becomes hot enough for He fusion. Fusion under degenerate conditions is unstable. Thus, there's runaway fusion:
 - "Helium Flash":
 - * $\uparrow T$ while $P = \text{const}$, so $\epsilon \uparrow$
 - * Yields $L \sim 10^{11} L_{\odot}$
 - * Contributes to the expansion of the envelope
 - * Next steps are dependent on metallicity:
 - Low metallicity stars go onto "Horizontal Branch"
 - High metallicity stars go to "Red Clump"

10.2.3 He Fusion:

This reaction is called the **triple- α reaction**: ${}^4\text{He} + {}^4\text{He} + {}^4\text{He} \rightarrow {}^{12}\text{C}$. The full reaction is:



Let's break this down:

1. Step (1): ${}^8\text{Be}$ decays into $2{}^4\text{He}$ rapidly, but if sufficiently high T ($\geq 10^8$ K), statistical thermal equilibrium can occur
2. Step (2): ${}^4\text{He}$ - ${}^8\text{Be}$ resonance causes fusion to excited state of ${}^{12}\text{C}$, ${}^{12}\text{C}^*$.
3. Step (3): ${}^{12}\text{C}^*$ mostly decays to ${}^8\text{Be} + {}^4\text{He}$ or $3{}^4\text{He}$, but sometimes to ${}^{12}\text{C} + [2\gamma \text{ or } (e^+ + e^-)]$. Statistical equilibrium eventually reached where $\frac{dn_{12}}{dt} = \frac{n_{12}}{t}$

Using the Saha method gives:

$$\epsilon = 5.4 \times 10^{11} \text{ erg/s/g} \frac{\rho^2 Y^3}{T_8^3} e^{-44/T_8}$$

where $Y \equiv \text{He}$ mass fraction and $\epsilon \propto \rho^\alpha T^\beta$ uses $\alpha = 2$, and $\beta = -3 + 44/T_8 \approx 24 - 40$.

Note that ${}^4\text{He} + {}^{12}\text{C} \rightarrow {}^{16}\text{O}$ at similar temperatures, so you normally get a mix of C and O .

10.2.4 End product of low mass stars:

- End product of stars with $0.5M_\odot \leq M \leq 8M_\odot$ is a C/O core with H- and He- burning shells.
- Star enters the “Asymptotic Giant Branch” as the convective envelope expands and the core contracts.
- The C/O core with $M \leq 1.4M_\odot$ becomes degenerate
- Envelope loses mass until left with a C/O white dwarf.

10.2.5 Mass Loss Mechanisms:

- Dust-driven winds
 - If $T \leq 3000$ K, solids can condense in the photosphere and be blown off by a high L . We can estimate \dot{M} by using momentum conservation:

$$\frac{L}{c} \sim \dot{M} v_{esc} \rightarrow \dot{M} = 10^{-5} M_\odot / \text{yr} \left(\frac{L}{10^4 L_\odot} \right)$$

for $v_{esc} \approx 30$ km/s

- Pulsations
 - He shell fusion is unstable and causes pulsations.
 - $\uparrow R$ means $\downarrow T$ and more material condenses.

10.2.6 White Dwarfs:

The core of a white dwarf is mostly He, or C and O.

- Stars with $M \leq 0.5M_\odot$
 - Do not have sufficient gravitational energy to heat up their core to the temperature required to ignite He fusion, and they will end up as He white dwarfs.
 - Lifetimes of these stars $\tau \geq \tau_{universe} \rightarrow$ He white dwarfs should not exist yet!
 - * Possible solution–binary evolution? Mass transfer happens before He ignition, so further evolution of the star is halted and that leaves the white dwarf made up mostly of He.
- Stars with $M \approx 1 - 8M_\odot$
 - Leaving a white dwarf with a CO core of mass $M \approx 0.6M_\odot$

Let's discuss the equilibrium structure of WDs. For a **non-relativistic degenerate electron gas**,

$$P = \frac{h^2}{5m_e} \left(\frac{3}{8\pi} \right)^{2/3} n^{5/3}$$

This can be rewritten as: $P = \frac{hP_F^2}{5m_eV}$, where $P_F = \left(\frac{3n}{8\pi} \right)^{1/3} h$. Since $n = \frac{\rho}{\mu_e m_p}$, $P = \frac{h^2}{5m_e} \left(\frac{3}{8\pi} \right)^{2/3} \frac{1}{(\mu_e m_p)^{5/3}} \rho^{5/3} = \kappa \rho^{5/3}$. So, NR WDs are well-described by $n = 3/2$ polytropes. Thus, we can use: $P_c = 0.77 \frac{GM^2}{R^4}$ and $\rho_c = 6\langle\rho\rangle = \frac{9M}{2\pi R^3}$.

$$\begin{aligned} \implies \kappa \rho_c^{5/3} &= 0.77 \frac{GM^2}{R^4} \implies \kappa \left(\frac{9}{2\pi} \right)^{5/3} \frac{M^{5/3}}{R^5} = 0.77 \frac{GM^2}{R^4} \\ \implies R &= 2.43 \frac{\kappa}{G} M^{-1/3} \end{aligned}$$

where $\kappa = 10^{13} \mu_e^{-5/3} \left(\frac{M}{m_e} \right)^{-1}$, and $\mu_e = 2$ for C/O.

$$\implies R = 0.013 R_\odot \left(\frac{M}{M_\odot} \right)^{-1/3} \left(\frac{\mu_e}{2} \right)^{-5/3} \left(\frac{m}{m_e} \right)^{-1}$$

This doesn't give a high enough central density or mass! (We need $\rho_c \sim 10^4 - 10^7$ g/cm³ and $M \sim 1M_\odot$, but we get $M \sim 1M_J$). Let's instead consider the structure of a **relativistic degenerate electron gas**.

For a relativistic degenerate electron gas,

$$P = \frac{hc}{4} \left(\frac{3}{8\pi} \right)^{1/3} n^{4/3} = \frac{hc}{4} \left(\frac{3}{8\pi} \right)^{1/3} \frac{1}{(\mu_e m_p)^{4/3}} \rho^{4/3}$$

So, relativistic WDs are well-described by $n = 3$ polytropes. Thus,

$$P_c = 11 \frac{GM^2}{R^4} = 30.4\kappa \frac{M^{4/3}}{R^4} \implies M^{2/3} = 2.76 \frac{\kappa}{G}$$

$$M = 1.45 M_\odot \left(\frac{M_e}{2} \right)^{-2}$$

This is the **Chandrasekhar Mass**. Note that the non-relativistic mass-radius relation is still valid for $M \leq 0.25 M_\odot$. WD (and NS) cannot have $M > M_{ch}$, since pressure needed to maintain HE ($P \propto \frac{M^2}{R^4}$) grows faster than pressure supplied by relativistic degeneracy pressure ($P \propto \frac{M^{4/3}}{R^4}$) for increasing M . If a WD accretes $M > M_{ch}$, it undergoes a runaway thermonuclear reaction (Type Ia SN).

10.2.7 White Dwarf Cooling:

WDs start with $T \approx 10^8$ K and cool over time. Since most mass is degenerate, conduction is very important for energy transport. Opacity for a degenerate gas is $\kappa_{degen} \sim \kappa_{classical} \left(\frac{E_F}{k_B T} \right)^{3/2}$:

$$\implies \kappa_{degen} = \kappa_{classical} \left(\frac{m_e c^2}{k_B T} \right)^{3/2} = 5000 T_8^{-3/2} \kappa_{classical} = \frac{\kappa^2 h^3 T n_i}{32 e^4 m_e^2}$$

WDs have no internal energy source but are born with thermal energy ($\sim N_i k_B T$) that can be radiated away. The timescale to redistribute energy in a WD interior is:

$$\tau_{cond} = \frac{N_i k_B T}{4\pi R^2 F} = \frac{N_i k_B T R}{4\pi R^2 \kappa T} = \frac{R^2}{(\kappa/n_i k_B)} \approx 5 \times 10^6 T_8^{-1} \text{ yrs}$$

(if we assume e^- scattering).

Degenerate cores become isothermal relatively rapidly. Core does not set rate at which energy leaves the object; the ENVELOPE sets the luminosity (non-degenerate layers).

Next, the WD becomes non-degenerate (ND), where $E_F \leq k_B T$, or $n \leq n_Q = \left(\frac{2\pi m_e k_B T}{h^2} \right)^{3/2} = 2 \times 10^{27} T_8^{3/2} \text{ cm}^{-3}$, or $\rho \leq 10^4 T_8^{3/2} \text{ g cm}^{-3}$. Since $\rho_c \approx 4 \times 10^6 \text{ g cm}^{-3} (M/M_\odot)^2$, most mass must be degenerate, with a thin ND surface layer. Assuming a radiative envelope:

$$\frac{dP}{dr} = -\rho g$$

$$F = \frac{L}{4\pi r^2} = \frac{-4}{3} \frac{1}{\kappa \rho} \frac{d}{dr} (\sigma_B T^4)$$

Assuming Kramer's opacity: $F = \frac{-4\sigma_B}{3} \frac{T^{7/2}}{\kappa_0 \rho^2} \frac{d}{dr} T^4 \propto \frac{g T^{7/2}}{\rho} \frac{dT^4}{d\rho}$. But, since $\rho \propto P/T$: $F \propto \frac{g T^{9/2}}{P} \frac{dT^4}{dP}$:

$$\begin{aligned} \implies PdP &\propto \frac{g}{F} T^{15/2} dT \\ \implies P^2 &\propto \frac{g}{F} T^{17/2} \\ \implies T &\propto P^{4/17} (g/F)^{-2/17} \\ \implies \rho &\propto T^{13/4} (g/F)^{1/2} \end{aligned}$$

We can now relate L to ρ and T using the photosphere, where $l = H$:

$$P_{ph} = \frac{g}{\kappa} \rightarrow \rho_{ph} = \frac{g}{\kappa k_B T_{eff}} \propto \frac{g T_{eff}^{5/2}}{\rho_{ph} k_B}$$